Syntheses and Spectroscopic and Quadratic Nonlinear Optical Properties of Extended Dipolar Complexes with Ruthenium(II) Ammine Electron Donor and *N*-Methylpyridinium Acceptor Groups

Benjamin J. Coe,*,† Lathe A. Jones,† James A. Harris,† Bruce S. Brunschwig,‡ Inge Asselberghs,§ Koen Clays,§ André Persoons,§,|| Javier Garín,# and Jesús Orduna#

Contribution from the Department of Chemistry, University of Manchester, Oxford Road, Manchester, United Kingdom M13 9PL, Chemistry Department, Brookhaven National Laboratory, P.O. Box 5000, Upton, New York 11973-5000, Laboratory of Chemical and Biological Dynamics, Center for Research on Molecular Electronics and Photonics, University of Leuven, Celestijnenlaan 200D, B-3001 Leuven, Belgium, Optical Sciences Center, University of Arizona, Tucson, Arizona, 85721, and Departamento de Química Orgánica, ICMA, Universidad de Zaragoza-CSIC, E-50009 Zaragoza, Spain

Received December 5, 2003; E-mail: b.coe@man.ac.uk.

Abstract: In this paper, we describe the extremely unusual optical properties of Ru^{II}-based electron donor–acceptor (D–A) polyene and some closely related chromophores. For three different polyene series, the intense, visible d→π* metal-to-ligand charge-transfer bands unexpectedly blue-shift as the number of *E*-ethylene units (*n*) increases from 1 to 3, and the static first hyperpolarizabilities β_0 determined via hyper-Rayleigh scattering and Stark spectroscopy maximize at $n = 2$, in marked contrast to other known D–A polyenes in which β_0 increases steadily with *n*. Time-dependent density-functional theory and finite field calculations verify these empirical trends, which arise from the orbital structures of the complexes. This study illustrates that transition metal-based nonlinear optical chromophores can show very different behavior when compared with their more thoroughly studied purely organic counterparts.

Introduction

Molecular materials which exhibit nonlinear optical (NLO) properties are of great current interest due to their potential utility in novel optoelectronic and photonic technologies.[1] The prospects for imminent applications are currently more promising for materials with quadratic (second-order) NLO effects, when compared with those displaying cubic (third-order) effects, although the two types of phenomena are not mutually exclusive. The design criteria for purely organic quadratic NLO materials are generally well established,[1] and the preparation of molecules having sufficiently large first hyperpolarizability coefficients β, which provide the molecular origins of such NLO effects, is

straightforward. Recent research has also shown that organo-transition metal complexes offer many exciting possibilities for the combination of NLO effects with other molecular electronic properties (e.g., redox or magnetic behavior) to produce novel multifunctional materials.[2] However, the study of the NLO behavior of such compounds is currently a considerably less mature field when compared with purely organic materials which have been scrutinized very extensively.

The majority of molecules having especially large β values comprise a strong electron donor (D) group connected to a strong electron acceptor (A) via a conjugated π-bridge. The

---

† University of Manchester.

‡ Brookhaven National Laboratory. (Present address: Molecular Materials Research Center, Beckman Institute, MC 139-74, California Institute of Technology, 1200 East California Blvd., Pasadena, CA 91125, USA).

§ University of Leuven.

|| University of Arizona.

Universidad de Zaragoza.

(1) (a) *Nonlinear Optical Properties of Organic Molecules and Crystals*; Chemla, D. S., Zyss, J., Eds.; Academic Press: Orlando, FL, 1987; Vols. 1 and 2. (b) *Molecular Nonlinear Optics: Materials, Physics and Devices*; Zyss, J., Ed.; Academic Press: Boston, 1994. (c) *Organic Nonlinear Optical Materials (Advances in Nonlinear Optics, Vol. 1.)*; Bosshard, Ch., Sutter, K., Prêtre, Ph., Hulliger, J., Flörsheimer, M., Kaatz, P., Günter, P., Eds.; Gordon & Breach: Amsterdam, The Netherlands, 1995. (d) *Nonlinear Optics of Organic Molecules and Polymers*; Nalwa, H. S., Miyata, S., Eds.; CRC Press: Boca Raton, FL, 1997.

(2) (a) Nalwa, H. S. *Appl. Organomet. Chem.* **1991**, *5*, 349−377. (b) Marder, S. R. In *Inorganic Materials*, 2nd ed.; Bruce, D. W.; O'Hare, D., Eds.; Wiley: Chichester, United Kingdom; 1992; pp. 121−169. (c) Kanis, D. R.; Ratner, M. A.; Marks, T. J. *Chem. Rev.* **1994**, *94*, 195−242. (d) Long, N. J. *Angew. Chem., Int. Ed. Engl.* **1995**, *34*, 21−38. (e) Whittall, I. R.; McDonagh, A. M.; Humphrey M. G.; Samoc, M. *Adv. Organomet. Chem.* **1998**, *42*, 291−362. (f) Whittall, I. R.; McDonagh, A. M.; Humphrey M. G.; Samoc, M. *Adv. Organomet. Chem.* **1998**, *43*, 349−405. (g) Heck, J.; Dabek, S.; Meyer-Friedrichsen, T.; Wong, H. *Coord. Chem. Rev.* **1999**, *190−192*, 1217−1254. (h) Gray, G. M.; Lawson, C. M. In *Optoelectronic Properties of Inorganic Compounds*; Roundhill, D. M., Fackler, J. P., Jr., Eds.; Plenum: New York, U.S.A., 1999; pp. 1−27. (i) Shi, S. In *Optoelectronic Properties of Inorganic Compounds*; Roundhill, D. M., Fackler, J. P., Jr., Eds.; Plenum: New York, U.S.A., 1999; pp 55−105. (j) Le Bozec, H.; Renouard, T. *Eur. J. Inorg. Chem.* **2000**, 229−239. (k) Barlow, S.; Marder, S. R. *Chem. Commun.* **2000**, 1555−1562. (l) Lacroix, P. G. *Eur. J. Inorg. Chem.* **2001**, 339−348. (m) Di Bella, S. *Chem. Soc. Rev.* **2001**, *30*, 355−366. (n) Coe, B. J. In *Comprehensive Coordination Chemistry II*; McCleverty J. A., Meyer, T. J., Eds.; Pergamon Press: Oxford, United Kingdom, 2004; Vol. 9, pp 621−687.

---

linear optical properties of such polarizable dipolar compounds are characterized by intense, low energy $D(\pi) \rightarrow A(\pi^*)$ charge-transfer (CT) transitions. According to a widely used simple two-state model (TSM) for such species,[3] the static first hyperpolarizability β_0 can be given by

$$\beta_0 = \frac{3\Delta\mu_{12}(\mu_{12})^2}{(E_{max})^2} \qquad (1)$$

where μ_{12} is the transition dipole moment, $\Delta\mu_{12}$ is the dipole moment change, and E_{max} is the maximal energy of the CT absorption.[4] β_0 is a measure of the intrinsic NLO response under nonresonant conditions, and is especially relevant to practical NLO applications where absorption must be avoided. Extending the length of a π-conjugated system generally increases $\Delta\mu_{12}$ and decreases E_{max}, and is hence one of the most commonly adopted approaches to increasing the β_0 responses of dipolar organic molecules.[1] D—A polyenes have therefore attracted considerable attention,[5] and have been found to possess some of the largest β_0 values known.[6] Most such studies have involved purely organic D and A groups, but those describing molecules containing metal centers (often ferrocenyl D groups) have also confirmed that polyene chain extension affords the expected increases in β_0.[7]

We have used hyper-Rayleigh scattering (HRS)[8] and Stark (electroabsorption)[9] measurements to probe the quadratic NLO properties of a range of ruthenium pyridyl ammine complexes.[10] Such chromophores can exhibit very large β_0 responses which are associated with intense, low energy metal-to-ligand CT (MLCT) transitions.[10] The MLCT absorption and NLO properties of these complexes are highly tunable, in accordance with the TSM, and can also be readily and reversibly switched via the $Ru^{III/II}$ redox couple.[11] Our previous studies with complexes *trans*-$[Ru^{II}(NH_3)_4(L^D)(L^A)]^{3+}$ (L^D = electron-rich ligand, L^A = pyridyl pyridinium ligand) have largely focused on increasing

the electron donating strength of the Ru^{II} center and the electron accepting ability of L^A. We have now also prepared and studied a number of complexes featuring extended π-conjugated bridges in order to investigate how this aspect of the molecular structure affects the linear and NLO properties of such chromophores. A limited number of the experimental results described herein have been previously communicated.[12]

Experimental Section

Materials and Procedures. All reactions were performed under an Ar atmosphere and in Ar-purged solvents. All reactions and chromatographic purifications involving complex salts were performed in the dark. Anhydrous THF was distilled from Na/benzophenone under Ar prior to use. The compounds (1,3-dioxolan-2-yl-methyl)tributyl phosphonium bromide,[13] 4-[E-2-(4-pyridyl)ethenyl]benzaldehyde,[14] $[Ru^{II}(NH_3)_5(H_2O)][PF_6]_2$,[15] *trans*-$[Ru^{III}(SO_4)(NH_3)_4(py)]Cl$ (py = pyridine),[15] *trans*-$[Ru^{III}(SO_4)(NH_3)_4(mim)]Cl$ (mim = *N*-methylimidazole)[10d] and $[MeQ^+]I$ (MeQ^+ = *N*-methyl-4,4′-bipyridinium)[10a] were synthesized by previously published methods. Products were dried overnight in a vacuum desiccator ($CaCl_2$) prior to characterization.

Physical Measurements. ^{1}H NMR spectra were recorded on a Varian XL-300 spectrometer and all chemical shifts are referenced to TMS. The fine splitting of pyridyl or phenyl ring AA′BB′ patterns is ignored and the signals are reported as simple doublets, with J values referring to the two most intense peaks. Elemental analyses were performed by the Microanalytical Laboratory, University of Manchester and UV—visible spectra were obtained by using a Hewlett-Packard 8452A diode array spectrophotometer. IR spectra were recorded as evaporated films from $CHCl_3$ between NaCl plates with a Perkin-Elmer RX-1 FTIR spectrometer and mass spectra were measured by using +electrospray on a Micromass Platform spectrometer with acetone as the solvent (cone voltage 30 V).

Cyclic voltammetric measurements were carried out by using an EG&G PAR model 283 potentiostat/galvanostat. A single-compartment cell was used with a silver/silver chloride reference electrode, a Pt disk working electrode and a Pt wire auxiliary electrode. Acetonitrile was freshly distilled (from CaH_2) and $[N(C_4H_9-n)_4]PF_6$, twice recrystallized from ethanol and dried in vacuo, was used as the supporting electrolyte. Solutions containing ca. 10^{-3} M analyte (0.1 M electrolyte) were deaerated by purging with N_2. All $E_{1/2}$ values were calculated from $(E_{pa} + E_{pc})/2$ at a scan rate of 200 mV s^{-1}.

Synthesis of $[MeQ^+]Cl$. Excess aqueous NH_4PF_6 (0.2 M) was added dropwise to a stirred solution of $[MeQ^+]I$ (800 mg, 2.68 mmol) in water (20 mL) at room temperature. The white precipitate was filtered off, washed with water, and dried. This solid was dissolved in acetone (20 mL) at room temperature and excess $[N(C_4H_9-n)_4]Cl$ (0.2 M in acetone) was added with stirring. The white precipitate was filtered off, washed with acetone then diethyl ether and dried: 475 mg, 81%; δ_H (D_2O)

(3) (a) Oudar, J. L.; Chemla, D. S. *J. Chem. Phys.* **1977**, *66*, 2664—2668. (b) Oudar, J. L. *J. Chem. Phys.* **1977**, *67*, 446—457.

(4) Note that the prefactor of 3 in eq 1 is not unique and that other two-state equations replace this factor by 6 or 3/2. See: Willetts, A.; Rice, J. E.; Burland, D. M.; Shelton, D. P. *J. Chem. Phys.* **1992**, *97*, 7590—7599.

(5) See for examples: (a) Marder, S. R.; Cheng, L.-T.; Tiemann, B. G.; Friedli, A. C.; Blanchard-Desce, M.; Perry, J. W.; Skindhøj, J. *Science* **1994**, *263*, 511—514. (b) Marder, S. R.; Gorman, C. B.; Meyers, F.; Perry, J. W.; Bourhill, G.; Brédas, J.-L.; Pierce, B. M. *Science* **1994**, *265*, 632—635. (c) Bublitz, G. U.; Ortiz, R.; Runser, C.; Fort, A.; Barzoukas, M.; Marder, S. R.; Boxer, S. G. *J. Am. Chem. Soc.* **1997**, *119*, 2311—2312. (d) Lawrentz, U.; Grahn, W.; Lukaszuk, K.; Klein, C.; Wortmann, R.; Feldner, A.; Scherer, D. *Chem. Eur. J.* **2002**, *8*, 1573—1590.

(6) Blanchard-Desce, M.; Alain, V.; Bedworth, P. V.; Marder, S. R.; Fort, A.; Runser, C.; Barzoukas, M.; Lebus, S.; Wortmann, R. *Chem. Eur. J.* **1997**, *3*, 1091—1104.

(7) See for examples: (a) Blanchard-Desce, M.; Runser, C.; Fort, A.; Barzoukas, M.; Lehn, J.-M.; Bloy, V.; Alain, V. *Chem. Phys.* **1995**, *199*, 253—261. (b) Alain, V.; Fort, A.; Barzoukas, M.; Chen, C.-T.; Blanchard-Desce, M.; Marder, S. R.; Perry, J. W. *Inorg. Chim. Acta* **1996**, *242*, 43—49. (c) Wu, Z.; Ortiz, R.; Fort, A.; Barzoukas, M.; Marder, S. R. *J. Organomet. Chem.* **1997**, *528*, 217—219. (d) Lee, I. S.; Seo, H.; Chung, Y. K. *Organometallics* **1999**, *18*, 1091—1096. (e) Jayaprakash, K. N.; Ray, P. C.; Matsuoka, I.; Bhadbhade, M. M.; Puranik, V. G.; Das, P. K.; Nishihara, H.; Sarkar, A. *Organometallics* **1999**, *18*, 3851—3858. (f) Farrell, T.; Meyer-Friedrichsen, T.; Malessa, M.; Haase, D.; Saak, W.; Asselberghs, I.; Wostyn, K.; Clays, K.; Persoons, A.; Heck, J.; Manning, A. R. *J. Chem. Soc., Dalton Trans.* **2001**, 29—36. (g) Farrell, T.; Manning, A. R.; Murphy, T. C.; Meyer-Friedrichsen, T.; Heck, J.; Asselberghs, I.; Persoons, A. *Eur. J. Inorg. Chem.* **2001**, 2365—2375.

(8) (a) Terhune, R. W.; Maker, P. D.; Savage, C. M. *Phys. Rev. Lett.* **1965**, *14*, 681—684. (b) Clays, K.; Persoons, A. *Rev. Sci. Instrum.* **1992**, *63*, 3285—3289. (c) Hendrickx, E.; Clays, K.; Persoons, A. *Acc. Chem. Res.* **1998**, *31*, 675—683.

(9) (a) Liptay, W. In *Excited States*, Vol. 1; Lim, E. C., Ed.; Academic Press: New York, 1974; pp. 129—229. (b) Bublitz, G. U.; Boxer, S. G. *Annu. Rev. Phys. Chem.* **1997**, *48*, 213—242.

(10) (a) Coe, B. J.; Chamberlain, M. C.; Essex-Lopresti, J. P.; Gaines, S.; Jeffery, J. C.; Houbrechts, S.; Persoons, A. *Inorg. Chem.* **1997**, *36*, 3284—3292. (b) Coe, B. J.; Essex-Lopresti, J. P.; Harris, J. A.; Houbrechts S.; Persoons, A. *Chem. Commun.* **1997**, 1645—1646. (c) Coe, B. J.; Harris, J. A.; Harrington, L. J.; Jeffery, J. C.; Rees, L. H.; Houbrechts S.; Persoons, A. *Inorg. Chem.* **1998**, *37*, 3391—3399. (d) Coe, B. J.; Harris, J. A.; Asselberghs, I.; Persoons, A.; Jeffery, J. C.; Rees, L. H.; Gelbrich T.; Hursthouse, M. B. *J. Chem. Soc., Dalton Trans.* **1999**, 3617—3625. (e) Coe, B. J.; Harris, J. A.; Clays, K.; Persoons, A.; Wostyn, K.; Brunschwig, B. S. *Chem. Commun.* **2001**, 1548—1549. (f) Coe, B. J.; Harris, J. A.; Brunschwig, B. S. *J. Phys. Chem. A* **2002**, *106*, 897—905. (g) Coe, B. J.; Jones, L. A.; Harris, J. A.; Sanderson, E. E.; Brunschwig, B. S.; Asselberghs, I.; Clays, K.; Persoons, A. *Dalton Trans.* **2003**, 2335—2341.

(11) (a) Coe, B. J.; Houbrechts, S.; Asselberghs I.; Persoons, A. *Angew. Chem. Int. Ed.* **1999**, *38*, 366—369. (b) Coe, B. J. *Chem. Eur. J.* **1999**, *5*, 2464—2471.

(12) Coe, B. J.; Jones, L. A.; Harris, J. A.; Brunschwig, B. S.; Asselberghs, I.; Clays, K.; Persoons, A. *J. Am. Chem. Soc.* **2003**, *125*, 862—863.

(13) Spangler, C. W.; McCoy, R. K. *Synth. Commun.* **1988**, *18*, 51—59.

(14) Ichimura, K.; Watanabe, S. *J. Polym. Sci., Polym. Chem.* **1982**, *20*, 1419—1432.

(15) Curtis, J. C.; Sullivan, B. P.; Meyer, T. J. *Inorg. Chem.* **1983**, *22*, 224—236.

8.89 (2 H, d, $J = 6.1$ Hz, C$_5$H$_4$N), 8.75 (2 H, d, $J = 5.3$ Hz, C$_5$H$_4$N), 8.36 (2 H, d, $J = 6.1$ Hz, C$_5$H$_4$N), 7.89 (2 H, d, $J = 5.3$ Hz, C$_5$H$_4$N), 4.38 (3 H, s, Me). Anal. Calcd for C$_{11}$H$_{11}$ClN$_2$·0.7H$_2$O: C, 60.25; H, 5.70; N, 12.77. Found: C, 60.45; H, 5.94; N, 12.68.

Synthesis of *E*-3-(4-Pyridyl)-2-propenal. A solution of (1,3-dioxolan-2-yl-methyl)tributyl phosphonium bromide (21.5 mL, 1.2 M in anhydrous THF, 25.8 mmol) and anhydrous THF (15 mL) was added dropwise to a mixture of NaH (1.4 g, 60% w/w dispersion in mineral oil, 35.0 mmol) and pyridine-4-carboxaldehyde (2.76 g, 25.8 mmol) in anhydrous THF (80 mL) at −5 °C over 2 h. The mixture was stirred for a further 30 min at room temperature before the dropwise addition of water (at 0 °C) to destroy unreacted NaH. A further 150 mL of water was added and the solution was extracted with CHCl$_3$ (4 × 100 mL). The extracts were evaporated to near dryness under reduced pressure and 1:1 2 M HCl/THF (80 mL) was added. After stirring at room temperature for 1 h, the solution was extracted with CHCl$_3$ (6 × 50 mL) and the extracts were discarded. The remaining aqueous phase was made basic by the addition of aqueous NaOH (4.0 M), until a pale precipitate formed (this occurred above pH 8.0), and the crude product was extracted into CHCl$_3$ (6 × 80 mL). Note that care must be taken to avoid adding too much base at this stage, or the suspension turns dark brown and the yield drops substantially. Purification was effected by column chromatography on silica gel (220−440 mesh). The column was packed with a CHCl$_3$ slurry and elution with THF: diethyl ether (1:10) gave a tan solid which was sublimed (90 °C, 3 mmHg) to afford white crystals: 1.65 g, 48%; δ_H (CDCl$_3$) 9.79 (1 H, d, $J = 7.4$ Hz, CH=O), 8.68 (2 H, d, $J = 6.2$ Hz, C$_5$H$_4$N), 7.44 (1 H, d, $J = 15.8$ Hz, CH), 7.39 (2 H, d, $J = 6.2$ Hz, C$_5$H$_4$N), 6.85 (1 H, dd, $J = 16.1$, 7.6 Hz, CH); ν(C=O) 1683 s cm^{-1}. Anal. Calcd for C$_8$H$_7$NO: C, 72.17; H, 5.30; N, 10.52. Found: C, 71.72; H, 5.36; N, 10.31.

Synthesis of *E,E*-5-(4-Pyridyl)penta-2,4-dienal. This compound was prepared from *E*-3-(4-pyridyl)propenal (1.50 g, 11.3 mmol), by using exactly the same conditions and purification procedure as described above, to afford a white solid: 1.44 g, 80%; δ_H (CDCl$_3$) 9.68 (1 H, d, 7.8 Hz, CH=O), 8.65 (2 H, d, $J = 6.2$ Hz, C$_5$H$_4$N), 7.37 (2 H, d, $J = 6.2$ Hz, C$_5$H$_4$N), 7.29 (1 H, dd, $J = 14.8$, 10.9 Hz, CH), 7.18 (1 H, dd, $J = 15.1$, 10.9 Hz, CH), 6.96 (1 H, d, $J = 15.0$ Hz, CH), 6.37 (1 H, dd, $J = 14.6$, 7.8 Hz, CH); ν(C=O) 1665 s cm^{-1}. Anal. Calcd for C$_{10}$H$_9$NO: C, 75.45; H, 5.70; N, 8.80. Found: C, 75.35; H, 5.79; N, 8.60.

Synthesis of *E,E,E*-7-(4-Pyridyl)hepta-2,4,6-trienal. This compound was prepared from *E,E*-5-(4-pyridyl)penta-2,4-dienal (1.00 g, 6.28 mmol), by using exactly the same conditions and purification procedure as described above, to afford a white solid: 0.95 g, 82%; δ_H (CDCl$_3$) 9.55 (1 H, d, 7.8 Hz, CH=O), 8.52 (2 H, d, $J = 6.2$ Hz, C$_5$H$_4$N), 7.23 (2 H, d, $J = 6.2$ Hz, C$_5$H$_4$N), 7.12 (1 H, dd, $J = 15.2$, 11.0 Hz, CH), 7.00 (1 H, dd, $J = 15.5$, 11.0 Hz, CH), 6.76 (1 H, dd, $J = 14.8$, 10.7 Hz, CH), 6.68−6.52 (2 H, m, CH), 6.18 (1 H, dd, $J = 15.3$, 7.8 Hz, CH); ν(C=O) 1675 s cm^{-1}. Anal. Calcd for C$_{12}$H$_{11}$NO: C, 77.81; H, 5.99; N, 7.56. Found: C, 78.02; H, 5.74; N, 7.67.

Synthesis of [*N*-Methyl-4-{*E,E*-4-(4-pyridyl)buta-1,3-dienyl}-pyridinium]X, [Mebpb$^+$]X (X = I$^-$, PF$_6^-$ or Cl$^-$). Piperidine (0.3 mL) was added to a solution of *E*-3-(4-pyridyl)propenal (2.00 g, 15.0 mmol) and *N*-methyl-4-picolinium iodide (3.53 g, 15.0 mmol) in ethanol (30 mL), and the solution was stirred at room temperature for 16 h. The pale yellow precipitate was filtered off, washed with ethanol then diethyl ether and dried: 657 mg, 12%; δ_H (CD$_3$OD) 8.77 (2 H, d, $J = 6.7$ Hz, C$_5$H$_4$N), 8.57 (2 H, d, $J = 6.2$ Hz, C$_5$H$_4$N), 8.16 (2 H, d, $J = 6.7$ Hz, C$_5$H$_4$N), 7.82 (1 H, dd, $J = 15.5$, 10.7 Hz, CH), 7.63 (2 H, d, $J = 6.2$ Hz, C$_5$H$_4$N), 7.52 (1 H, dd, $J = 15.5$, 10.7 Hz, CH), 7.12 (1 H, d, $J = 13.1$ Hz, CH), 7.10 (1 H, d, $J = 13.1$ Hz, CH), 4.92 (3 H, s, Me). Anal. Calcd for C$_{15}$H$_{15}$IN$_2$·H$_2$O: C, 48.93; H, 4.65; N, 7.61. Found: C, 48.96; H, 4.59; N, 7.66. Excess aqueous NH$_4$PF$_6$ (0.2 M) was added to a solution of [Mebpb$^+$]I·H$_2$O (600 mg, 1.63 mmol) in water (150 mL) at room temperature. The white precipitate of

[Mebpb$^+$]PF$_6$ was filtered off, washed with water, ethanol then diethyl ether and dried: 575 mg, 96%; δ_H (CD$_3$COCD$_3$) 8.94 (2 H, d, $J = 6.1$ Hz, C$_5$H$_4$N), 8.79 (2 H, d, $J = 6.7$ Hz, C$_5$H$_4$N), 8.30 (2 H, d, $J = 6.9$ Hz, C$_5$H$_4$N), 7.97 (1 H, dd, $J = 15.4$, 10.7 Hz, CH), 7.84 (2 H, d, $J = 6.2$ Hz, C$_5$H$_4$N), 7.73 (1 H, dd, $J = 15.7$, 10.7 Hz, CH), 7.38 (1 H, d, $J = 15.5$ Hz, CH), 7.30 (1 H, d, $J = 15.5$ Hz, CH), 4.54 (3 H, s, Me). Anal. Calcd for C$_{15}$H$_{15}$F$_6$N$_2$P: C, 48.93; H, 4.11; N, 7.61. [M−PF$_6^-$]$^+$ = 223. Found: C, 48.98; H, 3.94; N, 7.28. [M − PF$_6^-$]$^+$ = 223. Excess [N(C$_4$H$_9$-*n*)$_4$]Cl (0.2 M in acetone) was added to a stirred solution of [Mebpb$^+$]PF$_6$ (100 mg, 0.272 mmol) in acetone (5 mL) at room temperature. The white precipitate was filtered off, washed with acetone then diethyl ether and dried (note: the [Mebpb$^+$]Cl·2.1H$_2$O product is hygroscopic): 66 mg, 82%; δ_H (D$_2$O) 8.40 (2 H, d, $J = 6.3$ Hz, C$_5$H$_4$N), 8.34 (2 H, d, $J = 6.3$ Hz, C$_5$H$_4$N), 7.80 (2 H, d, $J = 6.3$ Hz, C$_5$H$_4$N), 7.48−7.40 (3 H, m, C$_5$H$_4$N and CH), 7.25 (1 H, dd, $J = 15.5$, 10.8 Hz, CH), 6.86 (1 H, d, $J = 15.5$ Hz, CH), 6.80 (1 H, d, $J = 15.5$ Hz, CH), 4.10 (3 H, s, Me). Anal. Calcd for C$_{15}$H$_{15}$ClN$_2$·2.1H$_2$O: C, 60.75; H, 6.53; N, 9.45. Found: C, 60.69; H, 6.02; N, 9.27.

Synthesis of [*N*-Methyl-4-{*E,E,E*-6-(4-pyridyl)hexa-1,3,5-trienyl}-pyridinium]X, [Mebph$^+$]X (X = I$^-$, PF$_6^-$ or Cl$^-$). [Mebph$^+$]I was prepared and isolated in the same manner as [Mebpb$^+$]I·H$_2$O, but using *E,E*-5-(4-pyridyl)penta-2,4-dienal (1.85 g, 11.6 mmol) and *N*-methyl-4-picolinium iodide (2.73 g, 11.6 mmol) in ethanol (50 mL). An orange solid was obtained: 1.6 g, 37%; δ_H (CD$_3$OD) 8.72 (2 H, d, $J = 6.9$ Hz, C$_5$H$_4$N), 8.52 (2 H, d, $J = 6.3$ Hz, C$_5$H$_4$N), 8.10 (2 H, d, $J = 6.9$ Hz, C$_5$H$_4$N), 7.75 (1 H, dd, $J = 15.4$, 10.7 Hz, CH), 7.57 (2 H, d, $J = 6.3$ Hz, C$_5$H$_4$N), 7.40 (1 H, dd, $J = 15.5$, 10.6 Hz, CH), 6.85−7.10 (4 H, m, CH), 4.34 (3 H, s, Me). Anal. Calcd for C$_{17}$H$_{17}$IN$_2$: C, 54.27; H, 4.55; N 7.45. Found: C, 53.89; H, 4.17; N, 6.99. [Mebph$^+$]PF$_6$· 5H$_2$O was prepared and isolated in the same manner as [Mebpb$^+$]PF$_6$, from [Mebph$^+$]I (200 mg, 0.53 mmol) to afford a yellow powder: 231 mg, 90%; δ_H (CD$_3$COCD$_3$) 8.91 (2 H, d, $J = 6.9$ Hz, C$_5$H$_4$N), 8.76 (2 H, d, $J = 6.5$ Hz, C$_5$H$_4$N), 8.23 (2 H, d, $J = 6.9$ Hz, C$_5$H$_4$N), 7.85 (2 H, d, $J = 6.5$ Hz, C$_5$H$_4$N), 7.81 (1 H, dd, $J = 15.7$, 10.0 Hz, CH), 7.61 (1 H, dd, $J = 15.7$, 10.2 Hz, CH), 6.96−6.94 (4 H, m, CH), 4.52 (3 H, s, Me). Anal. Calcd for C$_{17}$H$_{17}$F$_6$N$_2$P·5H$_2$O: C, 42.15; H, 5.62; N, 5.78. [M−PF$_6^-$]$^+$ = 249. Found: C, 41.85; H, 5.70; N, 5.60. [M−PF$_6^-$]$^+$ = 249. [Mebph$^+$]Cl·2.1H$_2$O was prepared and isolated in the same manner as [Mebpb$^+$]Cl·2.1H$_2$O, from [Mebph$^+$]PF$_6$·5H$_2$O (200 mg, 0.413 mmol) to afford yellow hygroscopic granules: 115 mg, 86%; δ_H (D$_2$O) 8.35−8.29 (4 H, m, C$_5$H$_4$N), 7.72 (2 H, d, $J = 6.6$ Hz, C$_5$H$_4$N), 7.56 (2 H, d, $J = 6.2$ Hz, C$_5$H$_4$N) 7.31 (1 H, dd, $J = 15.5$, 9.8 Hz, CH), 7.21 (1 H, dd, $J = 15.5$, 9.8 Hz, CH) 6.78−6.58 (4 H, m, CH), 4.03 (3 H, s, Me). Anal. Calcd for C$_{17}$H$_{17}$ClN$_2$·2.1H$_2$O: C, 63.29; H, 6.62; N, 8.68. Found: C, 63.11; H, 6.55; N, 8.44.

Synthesis of [*N*-Methyl-4-{*E,E,E*-8-(4-pyridyl)octa-1,3,5-tetra-enyl}pyridinium]PF$_6$, [Mebpo$^+$]PF$_6$. [Mebpo$^+$]I was prepared in the same manner as [Mebpb$^+$]I, but using *E,E,E*-7-(4-pyridyl)hepta-2,4,6-trienal (273 mg, 1.47 mmol), *N*-methyl-4-picolinium iodide (346 mg, 1.47 mmol) and piperidine (0.2 mL) in ethanol (5 mL). The poorly soluble resulting red solid was stirred in water (500 mL) at room temperature, the mixture was filtered to remove undissolved brown material, and excess aqueous NH$_4$PF$_6$ (0.2 M) was added to the filtrate. The orange precipitate was filtered off, washed with water, ethanol then diethyl ether and dried: 180 mg, 25%; δ_H (CD$_3$COCD$_3$) 8.91 (2 H, d, $J = 6.9$ Hz, C$_5$H$_4$N), 8.77 (2 H, d, $J = 6.6$ Hz, C$_5$H$_4$N), 8.23 (2 H, d, $J = 6.9$ Hz, C$_5$H$_4$N), 7.87 (2 H, d, $J = 6.6$ Hz, C$_5$H$_4$N), 7.82 (1 H, dd, $J = 15.4$, 10.6 Hz, CH), 7.65−7.54 (1 H, m, CH), 7.04−6.83 (6 H, m, CH), 4.54 (3 H, s, Me). Anal. Calcd for C$_{19}$H$_{19}$F$_6$N$_2$P·4H$_2$O: C, 46.35; H, 5.53; N, 5.69. [M−PF$_6^-$]$^+$ = 275. Found: C, 46.42; H, 4.17; N, 5.62. [M − PF$_6^-$]$^+$ = 275.

Synthesis of [*N*-Methyl-1,4-bis-{*E*-2-(4-pyridyl)ethenyl}benzene]X, [Mebpp$^+$]X (X = I$^-$, PF$_6^-$ or Cl$^-$). Piperidine (2 mL) was added to a solution of 4-[*E*-2-(4-pyridyl)ethenyl]benzaldehyde (440 mg, 2.10 mmol) and *N*-methyl-4-picolinium iodide (490 mg, 2.08 mmol) in ethanol (90 mL), and the solution was stirred at room temperature for

24 h. The yellow precipitate was filtered off, washed with ethanol and diethyl ether and dried: 200 mg, 22%; δ_H (CD$_3$OD) 8.76 (2 H, d, J = 6.9 Hz, C$_5$H$_4$N), 8.54 (2 H, d, J = 6.9 Hz, C$_5$H$_4$N), 8.22 (2 H, d, J = 6.9 Hz, C$_5$H$_4$N), 7.99 (1 H, d, J = 16.3 Hz, CH), 7.82 (2 H, d, J = 8.5 Hz, C$_6$H$_4$), 7.79 (2 H, d, J = 8.5 Hz, C$_6$H$_4$), 7.66 (2 H, d, J = 6.9 Hz, C$_5$H$_4$N), 7.60 (1 H, d, J = 16.3 Hz, CH), 7.52 (1 H, d, J = 16.5 Hz, CH), 7.35 (1 H, d, J = 16.3 Hz, CH), 4.36 (3 H, s, Me). Anal. Calcd for C$_{21}$H$_{19}$IN$_2$·H$_2$O: C, 56.77; H, 4.76; N, 6.30. Found: C, 57.01; H, 4.37; N, 6.23. Excess methanolic NH$_4$PF$_6$ (0.2 M) was added to a solution of [Mebpp$^+$]I·H$_2$O (300 mg, 0.675 mmol) in methanol (300 mL). The yellow precipitate of [Mebpp$^+$]PF$_6$ was filtered off, washed with methanol and dried: 218 mg, 73%; δ_H (CD$_3$COCD$_3$) 9.00 (2 H, d, J = 6.7 Hz, C$_5$H$_4$N), 8.63 (2 H, d, J = 6.0 Hz, C$_5$H$_4$N), 8.37 (2 H, d, J = 6.7 Hz, C$_5$H$_4$N), 8.10 (1 H, d, J = 16.3 Hz, CH), 7.88 (2 H, d, J = 8.7 Hz, C$_6$H$_4$), 7.84 (2 H, d, J = 8.7 Hz, C$_6$H$_4$), 7.64−7.69 (5 H, m, 3 × CH and C$_5$H$_4$N), 4.57 (3 H, s, Me). Anal. Calcd for C$_{21}$H$_{19}$F$_6$N$_2$P: C, 56.76; H, 4.31; N, 6.30. [M − PF$_6^-$]$^+$ = 299. Found: C, 56.35; H, 4.11; N, 5.96. [M − PF$_6^-$]$^+$ = 299. [Mebpp$^+$]Cl was prepared and isolated in the same manner as [Mebpp$^+$]Cl, from [Mebpp$^+$]PF$_6$ (100 mg, 0.225 mmol) to afford yellow hygroscopic granules: 71 mg, 89%; δ_H (D$_2$O) 9.00 (4 H, m, C$_5$H$_4$N), 7.75 (2 H, d, J = 6.7 Hz, C$_5$H$_4$N), 7.53 (1 H, d, J = 16.3 Hz, CH), 7.37 (4 H, s, C$_6$H$_4$), 7.10−6.83 (5 H, m, 3 × CH and C$_5$H$_4$N), 3.95 (3 H, s, Me). Anal. Calcd for C$_{21}$H$_{19}$ClN$_2$·H$_2$O: C, 71.48; H, 6.00; N. 7.94. Found: C, 71.02; H, 5.55; N, 8.33.

Synthesis of [Ru^{II}(NH$_3$)$_5$(Mebpb$^+$)](PF$_6$)$_3$ (3). A solution of [Ru^{II}(NH$_3$)$_5$(H$_2$O)](PF$_6$)$_2$ (110 mg, 0.222 mmol) and [Mebpb$^+$]PF$_6$ (93 mg, 0.253 mmol) in acetone (13 mL) was stirred at room temperature for 6 h. The resulting solution was loaded onto a column of silica gel (450 g, 220−440 mesh) packed with a CHCl$_3$ slurry, and eluted with 0.1 M NH$_4$PF$_6$ in methanol/acetone/acetonitrile (1:3:1). The most intense section of the major blue band was collected and diluted 5-fold with diethyl ether. The dark purple precipitate was filtered off, washed with a small amount of cold water, ethanol, then diethyl ether and dried: 73 mg, 39%; δ_H (CD$_3$COCD$_3$) 8.94 (2 H, d, J = 6.7 Hz, C$_5$H$_4$N), 8.87 (2 H, d, J = 6.6 Hz, C$_5$H$_4$N), 8.27 (2 H, d, J = 6.7 Hz, C$_5$H$_4$N), 7.87 (1 H, dd, J = 15.4, 10.9 Hz, CH), 7.68 (1 H, dd, J = 15.4, 10.7 Hz, CH), 7.47 (2 H, d, J = 6.6 Hz, C$_5$H$_4$N), 7.19 (1 H, d, J = 15.1 Hz, CH), 7.14 (1 H, d, J = 15.1 Hz, CH), 4.53 (3 H, s, Me), 3.33 (3 H, s, *trans*-NH$_3$), 2.66 (12 H, s, 4 × *cis*-NH$_3$). Anal. Calcd for C$_{15}$H$_{30}$F$_{18}$N$_7$P$_3$Ru: C, 21.34; H, 3.58; N 11.61. Found: C, 21.92; H, 3.43; N, 11.20.

Synthesis of [Ru^{II}(NH$_3$)$_5$(Mebph$^+$)](PF$_6$)$_3$ (4). This was prepared and purified in manner similar to **3** by using [Ru^{II}(NH$_3$)$_5$(H$_2$O)](PF$_6$)$_2$ (120 mg, 0.243 mmol) and [Mebph$^+$]PF$_6$·5H$_2$O (114 mg, 0.235 mmol) in acetone (15 mL) with a reaction time of 3 d. A dark purple solid was obtained: 20 mg, 10%; δ_H (CD$_3$COCD$_3$) 8.91 (2 H, d, J = 6.8 Hz, C$_5$H$_4$N), 8.82 (2 H, d, J = 6.6 Hz, C$_5$H$_4$N), 8.24 (2 H, d, J = 6.8 Hz, C$_5$H$_4$N), 7.83 (1 H, dd, J = 15.4, 10.1 Hz, CH), 7.55 (1 H, dd, J = 15.7, 9.9 Hz, CH), 7.43 (2 H, d, J = 6.6 Hz, C$_5$H$_4$N), 7.10−6.90 (4 H, m, CH), 4.53 (3 H, s, Me), 3.32 (3 H, s, *trans*-NH$_3$), 2.64 (12 H, s, 4 × *cis*-NH$_3$). Anal. Calcd for C$_{17}$H$_{32}$F$_{18}$N$_7$P$_3$Ru: C, 23.46; H, 3.71; N, 11.26. Found: C, 24.15; H, 3.50; N, 10.71.

Synthesis of [Ru^{II}(NH$_3$)$_5$(Mebpp$^+$)](PF$_6$)$_3$ (5). This was prepared and purified in manner similar to **4** by using [Ru^{II}(NH$_3$)$_5$(H$_2$O)](PF$_6$)$_2$ (111 mg, 0.225 mmol) and [Mebpp$^+$]PF$_6$ (100 mg, 0.225 mmol) in acetone (35 mL). A dark red solid was obtained: 88 mg, 42%; δ_H (CD$_3$COCD$_3$) 8.99 (2 H, d, J = 6.9 Hz, C$_5$H$_4$N), 8.83 (2 H, d, J = 6.7 Hz, C$_5$H$_4$N), 8.37 (2 H, d, J = 6.9 Hz, C$_5$H$_4$N), 8.10 (1 H, d, J = 16.4 Hz, CH), 7.88 (2 H, d, J = 8.8 Hz, C$_6$H$_4$), 7.83 (2 H, d, J = 8.8 Hz, C$_6$H$_4$), 7.74 (1 H, d, J = 16.5 Hz, CH), 7.67 (1 H, d, J = 16.3 Hz, CH), 7.55 (2 H, d, J = 6.7 Hz, C$_5$H$_4$N), 7.45 (1 H, d, J = 16.4 Hz, CH), 4.57 (3 H, s, Me), 3.28 (3 H, s, *trans*-NH$_3$), 2.67 (12 H, s, 4 × *cis*-NH$_3$). Anal. Calcd for C$_{21}$H$_{34}$F$_{18}$N$_7$P$_3$Ru: C, 27.40; H, 3.72; N, 10.65. Found: C, 27.73; H, 3.33; N, 10.22.

Synthesis of *trans*-[Ru^{II}(NH$_3$)$_4$(py)(MeQ$^+$)](PF$_6$)$_3$ (6). A solution of *trans*-[Ru^{III}(SO$_4$)(NH$_3$)$_4$(py)]Cl (212 mg, 0.558 mmol) in water (10

mL) was reduced over zinc amalgam (3 lumps) with Ar agitation for 20 min. This was filtered under Ar into a flask containing a solution of [MeQ$^+$]Cl·0.7H$_2$O (135 mg, 0.616 mmol) in water (10 mL) and the reaction was stirred at room temperature under Ar for 6 h. Excess aqueous NH$_4$PF$_6$ (0.2 M) was added to precipitate the crude product which was purified in manner similar to **3** to yield a dark red solid: 94 mg, 20%; δ_H (CD$_3$COCD$_3$) 9.19 (4 H, d, J = 6.6 Hz, C$_5$H$_4$N), 8.94 (2 H, d, J = 5.2 Hz, H^{2,6}), 8.75 (2 H, d, J = 6.9 Hz, C$_5$H$_4$N), 8.12 (2 H, d, J = 6.9 Hz, C$_5$H$_4$N), 8.02 (1 H, t, J = 6.9 Hz, H^4), 7.63 (2 H, t, J = 6.6 Hz, H^{3,5}), 4.66 (3 H, s, Me), 2.87 (12 H, s, 4 × NH$_3$). Anal. Calcd for C$_{16}$H$_{28}$F$_{18}$N$_7$P$_3$Ru: C, 22.49; H, 3.30; N, 11.48. Found: C, 22.95; H, 3.28; N, 11.21.

Synthesis of *trans*-[Ru^{II}(NH$_3$)$_4$(py)(Mebpb$^+$)](PF$_6$)$_3$ (8). This was prepared and purified in manner similar to **6** by using *trans*-[Ru^{III}(SO$_4$)(NH$_3$)$_4$(py)]Cl (171 mg, 0.450 mmol) in water (7 mL) and [Mebpb$^+$]Cl·2.1H$_2$O (116 mg, 0.391 mmol) in water (5 mL) with a reaction time of 24 h. A dark red solid was obtained: 100 mg, 28%; δ_H (CD$_3$COCD$_3$) 8.93 (2 H, d, J = 6.7 Hz, C$_5$H$_4$N), 8.88−8.83 (4 H, m, C$_5$H$_4$N and H^{2,6}), 8.25 (2 H, d, J = 6.9 Hz, C$_5$H$_4$N), 7.96−7.81 (2 H, m, CH and H^4), 7.66 (1 H, dd, J = 15.5, 10.9 Hz, CH), 7.63 (2 H, d, J = 6.3 Hz, C$_5$H$_4$N), 7.54 (2 H, t, J = 7.0 Hz, H^{3,5}), 7.17 (1 H, d, J = 15.4 Hz, CH), 7.16 (1 H, d, J = 15.4 Hz, CH), 4.54 (3 H, s, Me) 2.78 (12 H, s, 4 × NH$_3$). Anal. Calcd for C$_{20}$H$_{32}$F$_{18}$N$_7$P$_3$Ru: C, 26.50; H, 3.56; N, 10.82. Found: C, 26.85; H, 3.53; N, 10.26.

Synthesis of *trans*-[Ru^{II}(NH$_3$)$_4$(py)(Mebph$^+$)](PF$_6$)$_3$ (9). This was prepared and purified in manner similar to **6** by using *trans*-[Ru^{III}(SO$_4$)(NH$_3$)$_4$(py)]Cl (140 mg, 0.369 mmol) in water (6 mL) and [Mebph$^+$]Cl·2.1H$_2$O (105 mg, 0.325 mmol) in water (4 mL) with a reaction time of 3 d. A dark red solid was obtained: 52 mg, 17%; δ_H (CD$_3$COCD$_3$) 8.94−8.91 (4 H, m, C$_5$H$_4$N and H^{2,6}), 8.84 (2 H, d, J = 6.7 Hz, C$_5$H$_4$N), 8.25 (2 H, d, J = 6.7 Hz, C$_5$H$_4$N), 7.98 (1 H, m, H^4), 7.85 (1 H, dd, J = 15.7, 10.3 Hz, CH), 7.63−7.55 (5 H, m, C$_5$H$_4$N, CH and H^{3,5}), 7.09−6.93 (4 H, m, CH), 4.53 (3 H, s, Me), 2.83 (12 H, s, 4 × NH$_3$). Anal. Calcd for C$_{22}$H$_{34}$F$_{18}$N$_7$P$_3$Ru: C, 28.34; H, 3.68; N 10.51. Found: C, 28.95; H, 3.54; N, 10.14.

Synthesis of *trans*-[Ru^{II}(NH$_3$)$_4$(py)(Mebpp$^+$)](PF$_6$)$_3$ (10). This was prepared and purified in manner similar to **9** by using *trans*-[Ru^{III}(SO$_4$)(NH$_3$)$_4$(py)]Cl (209 mg, 0.550 mmol) and [Mebpp$^+$]Cl·H$_2$O (200 mg, 0.567 mmol) in water (45 mL). A dark red solid was obtained: 51 mg, 9%; δ_H (CD$_3$COCD$_3$) 8.98 (2 H, d, J = 6.7 Hz, C$_5$H$_4$N), 8.91 (2 H, d, J = 5.1 Hz, H^{2,6}), 8.85 (2 H, d, J = 6.6 Hz, C$_5$H$_4$N), 8.37 (2 H, d, J = 6.9 Hz, C$_5$H$_4$N), 8.11 (1 H, d, J = 16.3 Hz, CH), 7.98 (1 H, t, J = 7.6 Hz, H^4), 7.89 (2 H, d, J = 8.8 Hz, C$_6$H$_4$), 7.86 (2 H, d, J = 8.8 Hz, C$_6$H$_4$), 7.82−7.51 (7 H, m, 3 × CH, C$_5$H$_4$N and H^{3,5}), 4.57 (3 H, s, Me). Anal. Calcd for C$_{26}$H$_{36}$F$_{18}$N$_7$P$_3$Ru: C, 31.78; H, 3.69; N 9.98. Found: C, 31.87; H, 3.64; N, 9.46.

Synthesis of *trans*-[Ru^{II}(NH$_3$)$_4$(mim)(Mebpb$^+$)](PF$_6$)$_3$ (13). This was prepared and purified in manner similar to **6** by using *trans*-[Ru^{III}(SO$_4$)(NH$_3$)$_4$(mim)]Cl (92 mg, 0.240 mmol) in water (4 mL) and [Mebpb$^+$]Cl·2.1H$_2$O (62 mg, 0.209 mmol) in water (10 mL) with a reaction time of 12 h. A dark purple solid was obtained: 27 mg, 14%; δ_H (CD$_3$COCD$_3$) 8.96 (2 H, d, J = 6.7 Hz, C$_5$H$_4$N), 8.88 (2 H, d, J = 6.6 Hz, C$_5$H$_4$N), 8.27 (2 H, d, J = 6.7 Hz, C$_5$H$_4$N), 8.21 (1 H, s, C$_3$N$_2$H$_3$), 7.88 (1 H, dd, J = 15.4, 10.9 Hz, CH), 7.68 (1 H, dd, J = 15.4, 11.0 Hz, CH), 6.73 (2 H, d, J = 6.7 Hz, C$_5$H$_4$N), 7.49 (1 H, s, C$_3$N$_2$H$_3$), 7.39 (1 H, s, C$_3$N$_2$H$_3$), 7.18 (1 H, d, J = 15.4 Hz, CH), 7.17 (1 H, d, J = 15.4 Hz, CH), 4.54 (3 H, s, C$_5$H$_4$N−*Me*), 3.94 (3 H, s, C$_3$N$_2$H$_3$−*Me*), 2.68 (12 H, s, 4 × NH$_3$). Anal. Calcd for C$_{19}$H$_{33}$F$_{18}$N$_8$P$_3$Ru: C, 25.09; H, 3.66; N, 12.32. Found: C, 25.69; H, 3.24; N, 11.94.

Synthesis of *trans*-[Ru^{II}(NH$_3$)$_4$(mim)(Mebph$^+$)](PF$_6$)$_3$ (14). This was prepared and purified in manner similar to **9** by using *trans*-[Ru^{III}(SO$_4$)(NH$_3$)$_4$(mim)]Cl (153 mg, 0.400 mmol) in water (5 mL) and [Mebph$^+$]Cl·2.1H$_2$O (110 mg, 0.341 mmol) in water (10 mL). A dark purple solid was obtained: 67 mg, 21%; δ_H (CD$_3$COCD$_3$) 8.91 (2 H, d, J = 6.9 Hz, C$_5$H$_4$N), 8.82 (2 H, d, J = 5.7 Hz, C$_5$H$_4$N), 8.24 (2 H,

d, $J = 6.9$ Hz, C_5H_4N), 8.15 (1 H, s, $C_3N_2H_3$), 7.83 (1 H, dd, $J = 15.4$, 10.2 Hz, CH), 7.65–7.48 (4 H, m, CH, C_5H_4N and $C_3N_2H_3$), 7.37 (1 H, s, $C_3N_2H_3$), 7.08–6.94 (4 H, m, CH), 4.52 (3 H, s, C_5H_4N–*Me*), 3.95 (3 H, s, $C_3N_2H_3$–*Me*), 2.65 (12 H, s, 4 × NH_3). Anal. Calcd for $C_{21}H_{35}F_{18}N_8P_3Ru$: C, 26.96; H, 3.77; N, 11.98. Found: C, 27.20; H, 3.67; N, 11.41.

Synthesis of *trans*-[Ru^{II}(NH$_3$)$_4$(mim)(Mebpp$^+$)](PF$_6$)$_3$ (15). A solution of *trans*-[Ru^{III}(SO$_4$)(NH$_3$)$_4$(mim)]Cl (299 mg, 0.781 mmol) in water (15 mL) was reduced over zinc amalgam (3 lumps) with Ar agitation for 20 min. This was filtered under Ar into a flask containing a solution of [Mebpp$^+$]Cl·H$_2$O (263 mg, 0.745 mmol) in water (35 mL) and the solution was stirred at 35 °C for 5 d. The crude product was precipitated by addition of excess aqueous NH$_4$PF$_6$ (0.2 M) and purified on a silica gel column by using NH$_4$PF$_6$ in acetone (0.1 M) as the eluant. The first major purple band was collected and precipitated with a 5-fold excess of diethyl ether, then reprecipitated from acetone/diethyl ether to give a dark purple solid: 35 mg, 5%; δ_H (CD$_3$COCD$_3$) 8.98 (2 H, d, $J = 6.6$ Hz, C_5H_4N), 8.85 (2 H, d, $J = 5.8$ Hz, C_5H_4N), 8.37 (2 H, d, $J = 6.6$ Hz, C_5H_4N), 8.20 (1 H, s, $C_3N_2H_3$), 8.11 (1 H, d, $J = 16.3$ Hz, CH), 7.87 (4 H, s, C_6H_4), 7.78–7.52 (5 H, m, 3 × CH, C_5H_4N), 7.49 (1 H, s, $C_3N_2H_3$), 7.39 (1 H, s, $C_3N_2H_3$), 4.57 (3 H, s, C_5H_4N–*Me*), 3.95 (3 H, s, $C_3N_2H_3$–*Me*), 2.67 (12 H, s, 4 × NH_3). Anal. Calcd for $C_{25}H_{37}F_{18}N_8P_3Ru$: C, 30.47; H, 3.78; N, 11.37. Found: C, 31.15; H, 3.57; N, 10.88.

Hyper-Rayleigh Scattering. Details of the hyper-Rayleigh scattering (HRS) experiment have been discussed elsewhere,[8b,c,16] and the experimental procedure used was as previously described.[17] β values were determined by using the electric-field-induced second harmonic generation β_{1064} for *p*-nitroaniline (29.2 × 10^{-30} esu in acetonitrile)[18] as an external reference. All measurements were performed by using the 1064 nm fundamental of an injection-seeded, Q-switched Nd:YAG laser (Quanta-Ray GCR-5, 8 ns pulses, 7 mJ, 10 Hz). Dilute acetonitrile solutions (10^{-5}–10^{-6} M) were used to ensure a linear dependence of $I_{2\omega}/I_\omega^2$ on solute concentration, precluding the need for Lambert–Beer correction factors. Samples were filtered (Millipore, 0.45 μm), and none showed any fluorescence. One-dimensional hyperpolarizability is assumed, i.e. $\beta_{1064} = \beta_{333}$, and a relative error of ±15% is estimated.

Stark Spectroscopy. The electroabsorption apparatus, experimental methods and data analysis procedure were exactly as previously reported,[10f,19] with the only modification being that a xenon arc lamp was used as the light source in the place of a tungsten filament bulb. Butyronitrile was used as the glassing medium, for which the local field correction f_{int} is estimated as 1.33.[10f,19] The Stark spectrum for each compound was measured a minimum of three times using different field strengths, and the signal was always found to be quadratic in the applied field. A two-state analysis of an intramolecular CT (ICT) transition gives

$$\Delta\mu_{ab}^2 = \Delta\mu_{12}^2 + 4\mu_{12}^2 \tag{2}$$

where $\Delta\mu_{ab}$ is the dipole moment difference between the diabatic states, $\Delta\mu_{12}$ is the observed (adiabatic) dipole moment difference, and μ_{12} is the transition dipole moment. The latter can be determined from the oscillator strength f_{os} of the transition by

$$|\mu_{12}| = [f_{os}/(1.08 \times 10^{-5}E_{max})]^{1/2} \tag{3}$$

where E_{max} is the energy of the ICT maximum (in wavenumbers). The degree of delocalization c_b^2 and electronic coupling matrix element H_{ab}

for the diabatic states are given by

$$c_b^2 = \frac{1}{2}\left[1 - \left(\frac{\Delta\mu_{12}^2}{\Delta\mu_{12}^2 + 4\mu_{12}^2}\right)^{1/2}\right] \tag{4}$$

$$|H_{ab}| = \left|\frac{E_{max}(\mu_{12})}{\Delta\mu_{ab}}\right| \tag{5}$$

A relative error of ±20% is estimated for the β_0 values derived from the Stark data and using eq 1.

Computational Procedures. All theoretical calculations were performed by using the Gaussian 98[20] program. The molecular geometries were optimized assuming C_S symmetry using the hybrid functional B3P86[21] and the LanL2DZ[22] basis set. The same model chemistry was used for properties calculations. Electronic transitions were calculated by means of the TD-DFT method and the excited-state dipole moments were calculated by using the one particle RhoCI density. The default Gaussian 98 parameters were used in every case.

Results and Discussion

Molecular Design and Synthesis. We have synthesized seven new dipolar Ru^{II} complex salts in order to obtain data for three series in which the linkage between the coordinated pyridyl and *N*-methylpyridinium rings varies between 0 and 3 *E*-CH═CH units (Figure 1). The $n = 0$ or 1 complex salts featuring trans NH$_3$ or *N*-methylimidazole (mim) ligands (**1**, **2**, **11**, and **12**) are known,[10a,c,d] and form complete series with the new compounds **3**, **4**, **13**, and **14**. However, the $n = 0$ complex salt with a trans pyridine (py) ligand (**6**) is new and forms a series with the existing $n = 1$ analogue[10d] (**7**), **8**, and **9**. Three complex salts of a new ligand in which a *E,E*-1,4-bis(ethenyl)-phenylene group bridges the terminal rings (**5**, **10**, and **15**) have also been prepared to allow further comparisons with the related polyenyl species.

The new pyridyl polyene pro-ligand salts [Mebpb$^+$]I and [Mebph$^+$]I were synthesized via stepwise Wittig oxopropenyl-ations of pyridine-4-carboxaldehyde with (1,3-dioxolan-2-yl-methyl)tributyl phosphonium bromide,[13] followed by base-catalyzed condensations with *N*-methyl-4-picolinium iodide. This synthetic approach affords only the desired all-*E* products, although the isolated yields are low. The aldehyde intermediates *E*-3-(4-pyridyl)-2-propenal and *E,E*-5-(4-pyridyl)penta-2,4-dienal have been previously synthesized via other methods.[23] [Mebpb$^+$]I and [Mebph$^+$]I were metathesized to their Cl$^-$ or PF$_6^-$ salts for complexation reactions with the precursors

(16) Hendrickx, E.; Clays, K.; Persoons, A.; Dehu, C.; Brédas, J.-L. *J. Am. Chem. Soc.* **1995**, *117*, 3547–3555.

(17) Houbrechts, S.; Clays, K.; Persoons, A.; Pikramenou, Z.; Lehn, J.-M. *Chem. Phys. Lett.* **1996**, *258*, 485–489.

(18) Stähelin, M.; Burland, D. M.; Rice, J. E. *Chem. Phys. Lett.* **1992**, *191*, 245–250.

(19) Shin, Y. K.; Brunschwig, B. S.; Creutz, C.; Sutin, N. *J. Phys. Chem.* **1996**, *100*, 8157–8169.

(20) Frisch, M. J.; Trucks, G. W.; Schlegel, H. B.; Scuseria, G. E.; Robb, M. A.; Cheeseman, J. R.; Zakrzewski, V. G.; Montgomery, J. A., Jr.; Stratmann, R. E.; Burant, J. C.; Dapprich, S.; Millam, J. M.; Daniels, A. D.; Kudin, K. N.; Strain, M. C.; Farkas, O.; Tomasi, J.; Barone, V.; Cossi, M.; Cammi, R.; Mennucci, B.; Pomelli, C.; Adamo, C.; Clifford, S.; Ochterski, J.; Petersson, G. A.; Ayala, P. Y.; Cui, Q.; Morokuma, K.; Malick, D. K.; Rabuck, A. D.; Raghavachari, K.; Foresman, J. B.; Cioslowski, J.; Ortiz, J. V.; Baboul, A. G.; Stefanov, B. B.; Liu, G.; Liashenko, A.; Piskorz, P.; Komaromi, I.; Gomperts, R.; Martin, R. L.; Fox, D. J.; Keith, T.; Al-Laham, M. A.; Peng, C. Y.; Nanayakkara, A.; Gonzalez, C.; Challacombe, M.; Gill, P. M. W.; Johnson, B.; Chen, W.; Wong, M. W.; Andres, J. L.; González, C.; Head-Gordon, M.; Replogle, E. S.; Pople, J. A. GAUSSIAN 98, Revision A.7; Gaussian, Inc.: Pittsburgh, PA, 1998.

(21) The B3P86 Functional consists of Becke's three parameter hybrid functional (Becke, A. D. *J. Chem. Phys.* **1993**, *98*, 5648–5652) with the nonlocal correlation provided by the Perdew 86 expression: Perdew, J. P. *Phys. Rev. B* **1986**, *33*, 8822–8824.

(22) D95 on first row: Dunning, T. H.; Hay P. J. In *Modern Theoretical Chemistry*: Schaefer, H. F., III, Ed.; Plenum: New York, 1976, vol. 3, 1. Los Alamos ECP plus DZ on Na–Bi: (a) Hay, P. J.; Wadt, W. R. *J. Chem. Phys.* **1985**, *82*, 270–283. (b) Wadt, W. R.; Hay, P. J. *J. Chem. Phys.* **1985**, *82*, 284–298. (c) Hay, P. J.; Wadt, W. R. *J. Chem. Phys.* **1985**, *82*, 299–310.
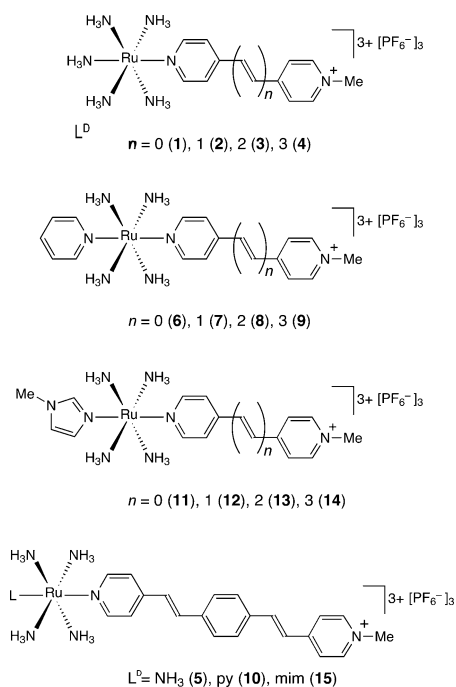
Figure 1. Chemical structures of the complex salts investigated.

Scheme 1

$[Ru^{II}(NH_3)_5(H_2O)][PF_6]_2$,[15] *trans*-$[Ru^{III}(SO_4)(NH_3)_4(py)]Cl$,[15] or *trans*-$[Ru^{III}(SO_4)(NH_3)_4(mim)]Cl$[10d] by using established coordination chemistry methods.[10a,c,d] The compound *E,E,E*-7-(4-pyridyl)hepta-2,4,6-trienal[24] was also prepared and used to synthesize the corresponding pro-ligand salt with four *E*-CH=CH bonds, [Mebpo+]I. However, we have unfortunately been unable to isolate any Ru^II complexes from the salt [Mebpo+]PF_6. Indeed, the reactivities of the new pyridyl polyene pro-ligands with $[Ru^{II}(NH_3)_5(H_2O)]^{2+}$ or *trans*-$[Ru^{II}L(NH_3)_4(H_2O)]^{2+}$ (L = py or mim) appear to decrease dramatically as the length of the polyene chain increases. Detailed UV–visible-based kinetic studies are underway in order to further investigate this interesting behavior.

The pro-ligand salt [Mebpp+]I was prepared by base-catalyzed condensation of 4-[*E*-2-(4-pyridyl)ethenyl]benzaldehyde[14] with *N*-methyl-4-picolinium iodide, and then converted into [Mebpp+]X (X = Cl⁻ or PF_6⁻) for complexation reactions. [Mebpp+]ClO_4 has been reported previously,[25] but the cation was prepared in that case via monomethylation of 1,4-bis[*E*-2-(4-pyridyl)ethenyl]benzene with dimethyl sulfate. The synthetic chemistry used to prepare the iodide salts of the new pro-ligand cations is summarized in Scheme 1.

Electronic Spectroscopy Studies. Electronic absorption spectra for the new complex salts **3–6**, **8–10**, and **13–15** were recorded in acetonitrile and the results are presented in Table 1. As expected, all of the complexes show intense d(Ru^II) → π*(L^A) MLCT bands, with λ_{max} values in the region 500–600 nm, which give rise to strong purple or blue colorations. Each complex also shows a single intense UV absorption due to
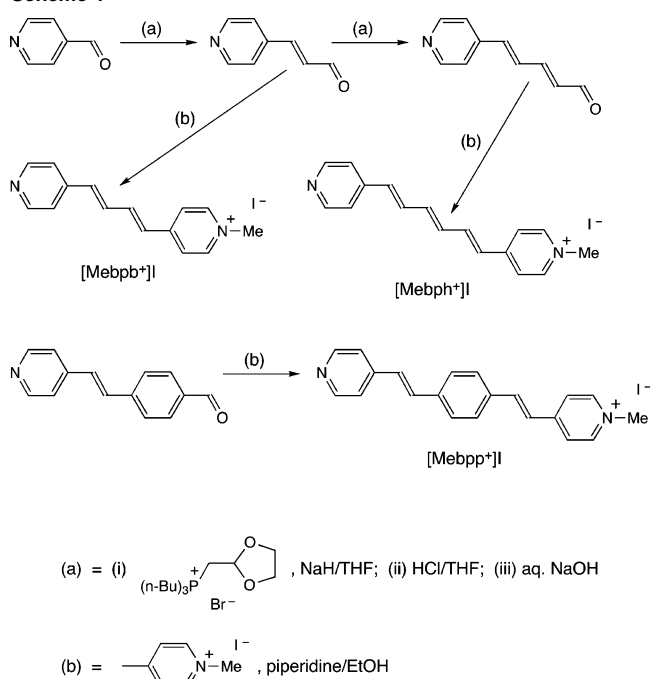
(23) Selected examples: (a) Huang, Y.-Z.; Shi, L.-L.; Yang, J.-H. *Tetrahedron Lett.* **1985**, *26*, 6447–6448. (b) Hagedorn, I.; Hohler, W. *Angew. Chem., Int. Ed. Engl.* **1975**, *14*, 486. (c) Tolbert, L. M.; Zhao, X.-D. *J. Am. Chem. Soc.* **1997**, *119*, 3253–3258. (d) Leitis, L.; Jansone, D.; Skolmeistere, R.; Popelis, J.; Gavars, M.; Shimanskaya, M. V.; Maslii, L. K.; Nikol'skaya, G. S. *Khim. Geterotsikl. Soedin.* **1991**, 77–80.
(24) (a) Duhamel, L.; Ple, G.; Ramondenc, Y. *Tetrahedron Lett.* **1989**, *30*, 7377–7380. (b) Ramondenc, Y.; Ple, G. *Tetrahedron* **1993**, *49*, 10 855–10 876.
(25) Kunitake, M.; Nasu, K.; Manabe, O.; Nakashima, N. *Bull. Chem. Soc. Jpn* **1994**, *67*, 375–378.

Table 1. Electrochemical and UV–Visible Data for the New Complex Salts *trans*-$[Ru^{II}(NH_3)_4(L^D)(L^A)](PF_6)_3{}^a$

| | | | E, V vs Ag–AgCl (ΔE_p, mV)[b] | | | |
salt	L^D	L^A	$E_{1/2}[Ru^{III/II}]$	$E_{1/2}[L^{A+/0,0/-}]$ or $E_{pc}{}^c$	λ_{max}, nm (ϵ, M⁻¹ cm⁻¹)[d]	assignment
3	NH_3	Mebpb+	0.45 (85)	−0.79	584 (18 700)	d → π*(Mebpb+)
					354 (32 600)	π → π*
4	NH_3	Mebph+	0.45 (75)	−0.77	568 (17 500)	d → π*(Mebph+)
					392 (39 700)	π → π*
5	NH_3	Mebpp+	0.45 (75)	−0.89	526 (19 400)	d → π*(Mebpp+)
					378 (44 000)	π → π*
6	py	MeQ+	0.69 (85)	−0.81 (100)	566 (17 200)	d → π*(MeQ+)
				−1.40 (110)	378 (5300)	d → π*(py)
					254 (17 700)	π → π*
8	py	Mebpb+	0.64 (85)	−0.75	552 (19 800)	d → π*(Mebpb+)
					356 (35 800)	π → π*
9	py	Mebph+	0.62 (85)	−0.76	542 (24 900)	d → π*(Mebph+)
					392 (51 100)	π → π*
10	py	Mebpp+	0.62 (90)	−0.90	510 (22 800)	d → π*(Mebpp+)
					378 (45 400)	π → π*
13	mim	Mebpb+	0.44 (85)	−0.77	592 (21 400)	d → π*(Mebpb+)
					352 (40 200)	π → π*
14	mim	Mebph+	0.45 (100)	−0.75	570 (21 900)	d → π*(Mebph+)
					392 (52 500)	π → π*
15	mim	Mebpp+	0.44 (95)	−0.88	520 (19 900)	d → π*(Mebpp+)
					376 (44 500)	π → π*

*^{a} Data for **3**, **4**, **13**, and **14** taken in part from ref 12. ^{b} Measured with solutions in (freshly distilled from CaH_2) acetonitrile ca. 10⁻³ M in analyte and 0.1 M in [N(C_4H_9-*n*)_4]PF_6 at a Pt disk working electrode with a scan rate of 200 mV s⁻¹. Ferrocene internal reference $E_{1/2}$ = 0.46 V, ΔE_p = 70 mV. ^{c} For an irreversible reduction process. ^{d} Measured with acetonitrile solutions ca. 5 × 10⁻⁵ M.*

π → π* intraligand CT (ILCT) excitations, which overlap the less intense d(Ru^II) → π*(py) MLCT bands in **8**, **9**, and **10**. These ILCT bands red-shift and gain intensity as *n* increases within the three series of polyene complex salts **1–4**, **6–9**, and **11–14**, and their energies are essentially independent of the nature of the trans ligand and also very similar to those observed for the corresponding pro-ligand salts.[26] Nonmethylated α,ω-dipyridyl polyenes also show intense π → π* bands in the 300–400 nm region which red-shift and gain intensity with increasing

Table 2. Electrochemical and Visible MLCT Absorption Data for Complex Salts **1**−**15**

salt	L^D	n	$\lambda_{max}{}^a$ (nm)	$E_{max}{}^a$ (eV)	$\epsilon_{max}{}^a$ (M^{-1} cm^{-1})	$E_{1/2}$[Ru$^{III/II}$]	$E_{1/2}$[L$^{+/0}$] or $E_{pc}{}^c$
1^d	NH$_3$	0	590	2.10	15 800	0.51 (75)	−0.86 (70)
2^e	NH$_3$	1	595	2.08	16 100	0.46 (70)	−0.80
3^f	NH$_3$	2	584	2.12	18 700	0.45 (85)	−0.79
4^f	NH$_3$	3	568	2.18	17 500	0.45 (75)	−0.77
5	NH$_3$		526	2.36	19 400	0.45 (75)	−0.89
6	py	0	566	2.19	17 200	0.69 (85)	−0.81 (100)
7^e	py	1	563	2.20	14 800	0.65 (70)	−0.75
8	py	2	552	2.25	19 800	0.64 (85)	−0.75
9	py	3	542	2.29	24 900	0.62 (85)	−0.76
10	py		510	2.46	22 800	0.62 (90)	−0.90
11^g	mim	0	602	2.06	16 200	0.52 (75)	−0.83 (70)
12^e	mim	1	604	2.05	16 200	0.47 (80)	−0.81
13^f	mim	2	592	2.09	21 400	0.44 (85)	−0.77
14^f	mim	3	570	2.18	21 900	0.45 (100)	−0.75
15	mim		520	2.38	19 900	0.44 (95)	−0.88

^{a} Measured with ca. 5 × 10^{-5} M solutions in acetonitrile at 298 K. ^{b} Measured with solutions in (freshly distilled from CaH$_2$) acetonitrile ca. 10^{-3} M in analyte and 0.1 M in [N(C$_4$H$_9$-n)$_4$]PF$_6$ at a Pt bead/disk working electrode with a scan rate of 200 mV s^{-1}. Ferrocene internal reference $E_{1/2}$ = 0.46 V, ΔE_p = 70 mV. ^{c} For an irreversible reduction process. ^{d} Ref 10c. ^{e} Ref 10d. ^{f} Data taken in part from ref 12. ^{g} Ref 10a.
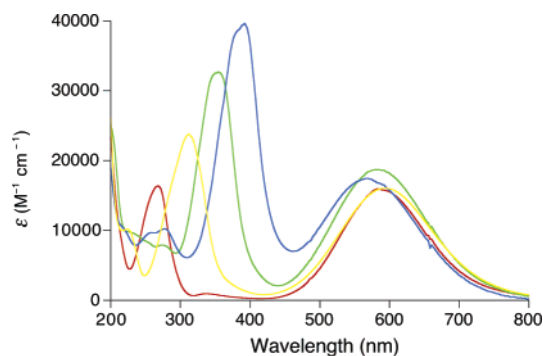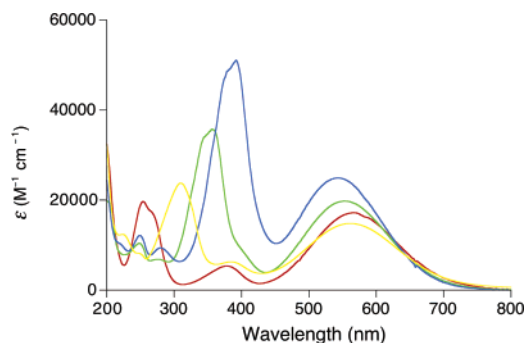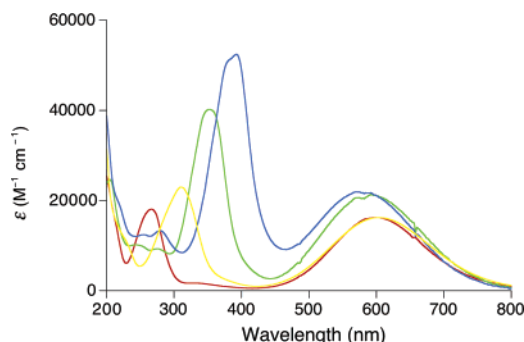

Figure 2. UV−visible absorption spectra of the complex salts **1** (red), **2** (yellow), **3** (green), and **4** (blue) at 298 K in acetonitrile.

Figure 3. UV−visible absorption spectra of the complex salts **6** (red), **7** (yellow), **8** (green), and **9** (blue) at 298 K in acetonitrile.

Figure 4. UV−visible absorption spectra of the complex salts **11** (red), **12** (yellow), **13** (green), and **14** (blue) at 298 K in acetonitrile.

n.[27] To a first approximation, it is reasonable to assume that the ILCT excitations in **1**−**4**, **6**−**9**, and **11**−**14** possess relatively limited CT character and will not therefore contribute substantially to the NLO responses which will be dominated by the lower energy and more strongly directional MLCT transitions (but see later). The MLCT data for the new complex salts are also collected in Table 2, together with those for the previously reported compounds **1**, **2**, **7**, **11**, and **12** for purposes of comparison. Representative UV−visible absorption spectra for the three series of polyene complex salts **1**−**4**, **6**−**9**, and **11**−**14** are shown in Figures 2-4.

The collected absorption data in Table 2 show that within each of the three separate polyene series, the E_{max} values change only slightly on moving from n = 0 to 1, but then increase as n increases further up to 3. The MLCT maxima hence shift to higher energy as the polyene chains are extended. This is a highly unusual result because the CT bands of D−A polyene chromophores almost invariably *red-shift* on chain elongation,

irrespective of whether terminal metal centers are present.[5−7] To our knowledge, the only previous reports of D−A polyenes in which the CT bands blue-shift with increasing the number of vinylenic spacer units involve several series of compounds containing tetrathiafulvalenyl (TTF) D groups in combination with various strong electron acceptors including 2,2-dicyanovinyl and 5-methylidene-1,3-diethyl-2-thiobarbituric acid.[28] Interestingly, related TTF compounds with 4-nitrophenyl A groups show more normal optical behavior.[29] D−A oligo-(phenylenevinylene) chromophores, in which the conjugated bridge contains alternating 1,4-phenylene rings and *E*-CH=CH units, can also display hypsochromic shifting of CT bands on extension of conjugation.[30] The blue-shifts of ca. 0.2 eV observed in the MLCT bands on moving from a *E,E,E*-1,3,5-hexatrienyl to a longer *E,E*-1,4-bis(ethenyl)phenylene bridge (i.e. **4** → **5**, **9** → **10**, or **14** → **15**) are consistent with results obtained with related purely organic compounds.[31]

(26) The absorption maxima for the PF$_6^-$ salts of the pyridyl pro-ligands are as follows (nm, in acetonitrile): 264 (n = 0), 316 (n = 1), 356 (n = 2), 394 (n = 3).

(27) Woitellier, S.; Launay, J. P.; Spangler, C. W. *Inorg. Chem.* **1989**, *28*, 758−762.

(28) (a) González, M.; Martín, N.; Segura, J. L.; Garín, J.; Orduna, J. *Tetrahedron Lett.* **1998**, *39*, 3269−3272. (b) Garín, J.; Orduna, J.; Rupérez, J. I.; Alcalá, R.; Villacampa, B.; Sánchez, C.; Martín, N.; Segura, J. L.; González, M. *Tetrahedron Lett.* **1998**, *39*, 3577−3580. (c) González, M.; Martín, N.; Segura, J. L.; Seoane, C.; Garín, J.; Orduna, J.; Alcalá, R.; Sánchez, C.; Villacampa, B. *Tetrahedron Lett.* **1999**, *40*, 8599−8602. (d) González, M.; Segura, J. L.; Seoane, C.; Martín, N.; Garín, J.; Orduna, J.; Alcalá, R.; Villacampa, B.; Hernández, V.; López Navarrete, J. T. *J. Org. Chem.* **2001**, *66*, 8872−8882. (e) Andreu, R.; Garín, J.; Orduna, J. *Tetrahedron* **2001**, *57*, 7883−7892.

(29) Bryce, M. R.; Green, A.; Moore, A. J.; Perepichka, D. F.; Batsanov, A. S.; Howard, J. A. K.; Ledoux-Rak, I.; González, M.; Martín, N.; Segura, J. L.; Garín, J.; Orduna, J.; Alcalá, R.; Villacampa, B. *Eur. J. Org. Chem.* **2001**, 1927−1935.

(30) (a) Meier, H.; Petermann, R.; Gerold, J. *Chem. Commun.* **1999**, 977−978. (b) Mata, J. A.; Uriel, S.; Llusar, R.; Peris, E. *Organometallics* **2000**, *19*, 3797−3802. (c) Meier, H.; Gerold, J.; Kolshorn, H.; Baumann, W.; Bletz, M. *Angew. Chem., Int. Ed.* **2002**, *41*, 292−295. (d) Meier, H.; Gerold, J.; Jacob, D. *Tetrahedron Lett.* **2003**, *44*, 1915−1918.

(31) (a) Alain, V.; Rédoglia, S.; Blanchard-Desce, M.; Lebus, S.; Lukaszuk, K.; Wortmann, R.; Gubler, U.; Bosshard, C.; Günter, P. *Chem. Phys.* **1999**, *245*, 51−71. (b) Luo, J.-D.; Hua, J.-L.; Qin, J.-G.; Cheng, J.-Q.; Shen, Y.-C.; Lu, Z.-H.; Wang, P.; Ye, C. *Chem. Commun.* **2001**, 171−172.

Table 3. MLCT Absorption, Stark Spectroscopic, and HRS Data for Complex Salts **1**−**15**

salt	L^D	n	$\lambda_{max}{}^a$ (nm)	$E_{max}{}^a$ (eV)	$f_{os}{}^a$	$\mu_{12}{}^b$ (D)	$\Delta\mu_{12}{}^c$ (D)	$\Delta\mu_{ab}{}^d$ (D)	$c_b{}^{2\,e}$	$H_{ab}{}^f$ (cm^{-1})	$\beta_0[S]^g$ (10^{-30} esu)	$\beta_{1064}{}^h$ (10^{-30} esu)	$\beta_0[H]^i$ (10^{-30} esu)
1[j,k]	NH_3	0	645	1.92	0.20	5.2	13.8	17.3	0.10	4700	120	750	123
2[j,l]	NH_3	1	681	1.82	0.23	5.5	16.2	19.6	0.09	4100	175	828	142
3[m]	NH_3	2	675	1.84	0.43	7.9	22.4	27.4	0.09	4300	482	2593	372
4[m]	NH_3	3	669	1.85	0.36	7.2	27.1	30.6	0.06	3500	475	1308	131
5	NH_3		610	2.03	0.36	6.8	28.3	31.4	0.05	3600	373	1116	19[n]
6	py	0	611	2.03	0.29	6.1	16.2	20.3	0.10	4900	171	899	85
7[j,l]	py	1	638	1.94	0.25	6.0	19.3	22.7	0.08	4100	218	904	78[n]
8	py	2	631	1.97	0.50	8.2	25.1	30.0	0.08	4300	514	1332	75[n]
9	py	3	625	1.98	0.36	7.0	28.6	31.8	0.05	3500	412	1519	43[n]
10	py		573	2.16	0.41	7.0	27.8	31.1	0.05	3900	343	1404	88[n]
11[j,o]	mim	0	658	1.88	0.22	5.5	17.1	20.3	0.08	4100	170	523	100
12[j,l]	mim	1	687	1.80	0.26	6.3	18.0	22.0	0.09	4200	256	857	168
13[m]	mim	2	684	1.81	0.48	8.4	23.3	28.7	0.09	4300	586	1440	237
14[m]	mim	3	678	1.83	0.42	7.8	26.7	30.9	0.07	3700	563	1660	175
15	mim		610	2.03	0.36	6.8	30.1	33.1	0.04	3400	397	1358	46[n]

[a] Measured in butyronitrile glasses at 77 K (f_{os} is the oscillator strength determined by numerical integration of the digitized spectra). [b] Calculated from eq 3. [c] Calculated from $f_{int}\Delta\mu_{12}$ using $f_{int} = 1.33$. [d] Calculated from eq 2. [e] Calculated from eq 4. [f] Calculated from eq 5. [g] Calculated from eq 1. [h] Obtained from 1064 nm HRS measurements in acetonitrile solutions at 298 K. [i] Derived from β_{1064} by application of the TSM,[3] and assuming that the MLCT transition is dominant. [j] Ref 10f. [k] Ref 10c. [l] Ref 10d. [m] Data taken in part from ref 12. [n] Underestimated due to close proximity of λ_{max} to 532 nm. [o] Ref 10a.

Electrochemical Studies. The new complex salts **3**−**6**, **8**−**10**, and **13**−**15** were investigated via cyclic voltammetry in acetonitrile and the results are presented in Table 1, and also collected in Table 2. All of the complexes exhibit reversible or quasi-reversible Ru$^{III/II}$ oxidation waves. Within each of the polyene series, the Ru$^{III/II}$ $E_{1/2}$ values decrease by ca. 50 mV on moving from $n = 0$ to 1, indicating that the Ru centers become more electron rich due to the mildly electron donating influence of the 4-vinyl groups. However, further extension of the conjugated bridges leads to only small changes in the Ru$^{III/II}$ potentials. The pyridinium ligand first reduction waves are reversible only for $n = 0$, even up to scan rates as high as 200 V s^{-1}. Although correlation between the MLCT energies and the redox potentials is hence not possible, it can be concluded that variations in the ligand-based LUMO energies are primarily responsible for the observed changes in the MLCT energies on moving from $n = 1$ to 3. The E_{pc} values for **5**, **10**, and **15** are considerably negatively shifted with respect to those for their $n = 3$ counterparts, in keeping with the observed blue-shifts in the MLCT bands.

Hyper-Rayleigh Scattering Studies. The molecular first hyperpolarizabilities of complex salts **3**−**6**, **8**−**10**, and **13**−**15** were measured in acetonitrile solutions by using the HRS technique[8,16,17] with a 1064 nm Nd:YAG laser fundamental. The resulting resonance enhanced β_{1064} values were used to derive estimated static hyperpolarizabilities $\beta_0[H]$ by application of the TSM,[3] assuming that the MLCT bands dominate the NLO responses. The results are given in Table 3, together with previously reported data.[10a,c,d,12]

Unfortunately, because the TSM leads to underestimations of β_0 when the CT absorption maximum is located close to the second harmonic wavelength of 532 nm, the $\beta_0[H]$ data for the py complex salts are of little utility and do not afford any meaningful insights into the effects of extension of the conjugated system. However, the data for both of the other polyene series show that $\beta_0[H]$ maximizes at $n = 2$, and the values for $n = 3$ are similar to those for $n = 1$. The decrease in $\beta_0[H]$ on moving from $n = 2$ to 3 is somewhat larger for the pentaammine series. The underestimation effect is also found in the $\beta_0[H]$ values for **5**, **10**, and **15**. Although HRS is a very useful technique, the results given here demonstrate that

resonance effects can hinder its ability to afford structure−activity relationships for static first hyperpolarizabilities. We have hence also carried out Stark spectroscopic measurements as an alternative approach to deriving β_0 values and other molecular electronic parameters, having the advantage over HRS that resonance effects can be ignored.

Stark Spectroscopic Studies. All of the new complex salts **3**−**6**, **8**−**10**, and **13**−**15** were studied by electronic Stark effect spectroscopy in butyronitrile glasses at 77 K and the results are presented in Table 3, together with previously reported data.[10f,12] As found previously with related Ru^{II} ammine complexes,[10f,19] the electroabsorption spectra of **3**−**6**, **8**−**10**, and **13**−**15** were successfully modeled in terms of a large second derivative term, a small first derivative component and a negligible zeroth derivative contribution.

In all cases, the MLCT bands undergo marked red-shifts in the 77 K glass, as observed previously in related compounds.[10f,19] Although the same general trend in the variation of E_{max} with increasing n is evident in either medium, the form of this trend varies. At 298 K in acetonitrile, the decreases in E_{max} on moving from $n = 0$ to $n = 1$ are only slight, while the subsequent increases up to $n = 3$ are larger. The reverse pattern is observed at 77 K in butyronitrile, i.e. relatively large decreases in E_{max}, followed by small increases. Within each polyene series, $\Delta\mu_{12}$ increases steadily with n, as is normally observed for D−A polyenes, while μ_{12} is maximized at $n = 2$. As also observed in related compounds,[10f] the $\Delta\mu_{ab}$ values are considerably larger than their adiabatic counterparts. The magnitude of $c_b{}^2$ reflects the degree of mixing between the diabatic states, and the observed values of ≤ 0.1 are indicative of a limited degree of delocalization, consistent with the assignment of the visible absorptions as arising from MLCT transitions. Within the three polyene series **1**−**4**, **6**−**9**, and **11**−**14**, the values of $c_b{}^2$ and H_{ab} decrease on moving from $n = 2$ to 3, indicating a decreasing extent of orbital overlap between the Ru^{II} electron donor and N-methylpyridinium electron acceptor groups. The fact that both $c_b{}^2$ and H_{ab} have their lowest values in the $n = 3$ and E,E-1,4-bis(ethenyl)phenylene-bridged compounds is entirely logical because these species contain the longest conjugated bridges.

Most importantly, the values of $\beta_0[S]$, derived by using eq 1, also show remarkably consistent behavior within each series;

Table 4. ILCT Absorption and Stark Spectroscopic Data for Complex Salts **3**−**5**, **8**−**10**, and **13**−**15**

salt	L^D	n	$\lambda_{max}{}^a$ (nm)	$E_{max}{}^a$ (eV)	$f_{os}{}^a$	$\mu_{12}{}^b$ (D)	$\Delta\mu_{12}{}^c$ (D)	$\Delta\mu_{ab}{}^d$ (D)	$c_b{}^{2}{}^e$	$H_{ab}{}^f$ (cm^{-1})	$\beta_0[S]_{ILCT}{}^g$ (10^{-30} esu)	$\beta_0[S]_{MLCT}{}^g$ (10^{-30} esu)	$\beta_0[S]_{TOT}{}^h$ (10^{-30} esu)
3	NH_3	2	377	3.29	0.58	6.8	12.7	18.6	0.16	9700	64	482	546
4	NH_3	3	408	3.04	0.63	7.4	14.5	20.8	0.15	8700	101	475	576
5	NH_3		385	3.22	0.91	8.6	13.6	21.9	0.19	10 200	113	373	486
8	py	2	370	3.35	0.52	6.5	11.7	17.4	0.16	10 000	51	514	565
9	py	3	404	3.07	1.00	9.3	12.5	22.4	0.22	10 300	134	412	546
10	py		403	3.08	0.97	9.1	11.8	21.7	0.23	10 400	121	343	464
13	mim	2	374	3.32	0.42	5.8	16.4	20.1	0.09	7700	59	586	645
14	mim	3	408	3.04	0.66	7.6	13.0	20.0	0.18	9300	95	563	658
15	mim		385	3.22	0.72	7.7	13.7	20.6	0.17	9700	91	397	488

[a] Measured in butyronitrile glasses at 77 K (f_{os} is the oscillator strength determined by numerical integration of the digitized spectra). [b] Calculated from eq 3. [c] Calculated from $f_{int}\Delta\mu_{12}$ using $f_{int} = 1.33$. [d] Calculated from eq 2. [e] Calculated from eq 4. [f] Calculated from eq 5. [g] Calculated from eq 1. [h] Sum of the $\beta_0[S]$ values for the two absorption bands, i.e. $\beta_0[S]_{ILCT} + \beta_0[S]_{MLCT}$.

$\beta_0[S]$ increases on moving from $n = 0$ to $n = 1$, shows a further dramatic increase to $n = 2$, and then decreases. Note however that this decrease in $\beta_0[S]$ is only experimentally significant for the py series. The $\beta_0[S]$ values are of similar magnitude, but generally substantially larger than those derived from the HRS measurements. This result is apparently consistent with the red-shifts in the MLCT bands on moving from solution to glass. However, because other two-state equations are available which would change the calculated $\beta_0[S]$ values by constant factors of either 2 or 0.5,[4] direct comparisons between the two sets of β_0 data should be made only with caution. What is most significant is that the trends shown in $\beta_0[S]$ are broadly the same as those found in $\beta_0[H]$, although the increase in $\beta_0[H]$ on moving from $n = 1$ to $n = 2$ is considerably smaller than that observed in the $\beta_0[S]$ values for the mim complexes. Since the $\beta_0[H]$ values for **5**, **10**, and **15** are clearly of little validity, it is satisfying to note that the $\beta_0[S]$ data for these compounds appear to be entirely reasonable. In each case, $\beta_0[S]$ is smaller than that of the analogous $n = 3$ compound, and this result can be traced largely to the corresponding increases of ca. 0.2 eV in E_{max} accompanied by decreases in μ_{12} which more than offset the slightly larger $\Delta\mu_{12}$ values. Nevertheless, the $\beta_0[S]$ values for **5**, **10**, and **15** are still very large and have been achieved with considerable gains in visible transparency, since the MLCT bands of these chromophores are somewhat higher in energy even than those of their $n = 0$ counterparts.

Figures 2−4 show that within the three polyene series, a clear trend in the high energy ILCT bands is also evident. As noted earlier, these absorptions red-shift and gain intensity steadily as n increases, such that they become particularly significant for the $n = 2$ or 3 complex chromophores. The question hence arises as to whether the potential contributions of these excitations to the quadratic NLO responses can be ignored, as has been the case thus far (and in our previous report).[12] Unfortunately, our Stark setup does not allow the ILCT bands for the $n = 0$ or 1 compounds to be analyzed, since it has an operational short wavelength limit of ca. 350 nm. This cutoff arises from several factors including the intensity of the light source, detector sensitivity and excessive near-UV absorption by the ITO glass windows used in the Stark cell. However, data for the ILCT bands have been obtained for the $n = 2$ or 3 chromophores and also for the complexes of the Mebpp$^+$ ligand. The data shown in Table 4 reveal that the ILCT bands do indeed possess relatively large $\Delta\mu_{12}$ values which lie in the range 40−70% of those for the corresponding MLCT transitions. Application of eq 1 then affords $\beta_0[S]_{ILCT}$ values of ca. 50 for the

$n = 2$ compounds and ca. 100 for their $n = 3$ counterparts. Summation of the two individual $\beta_0[S]$ values indicates that the total responses for the $n = 2$ or 3 chromophores are very similar and show no convincing evidence for either a decrease or an increase. These results indicate that the ILCT transitions contribute ca. 10% of the overall NLO responses of the $n = 2$ compounds but ca. 20% for their $n = 3$ analogues. It can be assumed that the corresponding relative contributions in the $n = 0$ or 1 chromophores will be ≤5%, so our previous assumption that only the MLCT bands need to be considered in these cases is reasonable.[10f]

The observation that both MLCT and ILCT transitions contribute to the NLO responses of our complex chromophores is in some respects reminiscent of the results reported previously for ferrocenyl-containing D-π−A compounds.[32] Such complexes also display two absorptions in the region 300−900 nm, with the higher energy (HE) band having greater intensity than that at lower energy (LE). However, in polyene derivatives bearing terminal strongly electron accepting groups both bands red-shift as n increases, although the HE band shifts more than the LE one.[7b] The electronic structures of such ferrocenyl derivatives have provoked some controversy; Kanis et al. claimed that the LE bands are ligand-field-based and the NLO responses are dominated by the HE bands which were assigned as being of MLCT character.[33] However, Calabrese et al. have assigned the LE bands as being of MLCT type and the HE bands as predominantly ILCT in nature, but with some metal character.[34] In keeping with the latter model, recent Stark spectroscopic studies show that both bands have large $\Delta\mu_{12}$ values.[32] An octamethylferrocenyl complex with a 1-dioxothia-3-(dicyanomethylene)inden-2-yl electron acceptor and a E,E,E-hexa-1,3,5-trienyl bridge has respective $\Delta\mu_{12}$ values of ca. 18 and 9 D for the LE and HE bands.[32] In this chromophore, application of the TSM indicates that the HE transition is responsible for ca. 25% of the β response, while the LE transition contributes 75%. Interestingly, in the compound 4-{E,E-4-(ferrocenyl)buta-1,3-dienyl}nitrobenzene, which contains a shorter conjugated bridge, the HE transition was found to dominate the TSM response, with a ca. 63% contribution.[32] In contrast, the electronic structures of our Ru^{II} compounds are more readily understood and show an increasing contribution of the ILCT

(32) Barlow, S.; Bunting, H. E.; Ringham, C.; Green, J. C.; Bublitz, G. U.; Boxer, S. G.; Perry, J. W.; Marder, S. R. *J. Am. Chem. Soc.* **1999**, *121*, 3715−3723.
(33) Kanis, D. R.; Ratner, M. A.; Marks, T. J. *J. Am. Chem. Soc.* **1992**, *114*, 10 338−10 357.
(34) Calabrese, J. C.; Cheng, L.-T.; Green, J. C.; Marder, S. R.; Tam, W. *J. Am. Chem. Soc.* **1991**, *113*, 7227−7232.
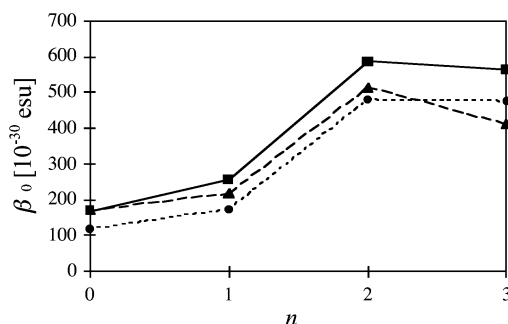
Figure 5. Stark-derived β_0 values as a function of n (only dominant MLCT transitions considered). - - -●- - - = NH$_3$ series (**1**−**4**); − −▲− − = py series (**6**−**9**); −■− = mim series (**11**−**14**).

transitions to the NLO response as the conjugated path length is extended.

Static First Hyperpolarizability Trends. The HRS data indicate that β_0 in these complex chromophores is effectively maximized at $n = 2$. The β_0 values derived by using Stark spectroscopic data for the MLCT bands mirror this trend (Figure 5), and no evidence for significant further increases for $n = 3$ is observed even when the contributions of the ILCT transitions are included in the Stark analysis. Kanis et al. have used ZINDO-SOS calculations on the hypothetical series of pyridyl carbonyl complexes Cr(CO)$_5${NC$_5$H$_4$-4-E-(CH=CH)$_n$-C$_6$H$_4$-4-CHO} to predict that the β_{vec} response (the vector component of β along the dipole moment direction) reaches a maximum for $n = 1$ and then decreases sharply up to $n = 3$.[35] This behavior is clearly very different to that found in purely organic polyenes, and was rationalized based on the fact that a pyridyl-coordinated metal center acts as both a π-donor and a σ-acceptor, and the primary acceptor of charge from the metal d-orbitals is actually the pyridyl ring, not the remote formyl group.[35] Perhaps surprisingly, no other theoretical or empirical studies have appeared since to test this conclusion. Our experimental results are in agreement with the theoretical predictions of Kanis et al. inasmuch as the extension of the polyene bridges does not lead to continual increases in the quadratic molecular NLO response. However, the prediction that β_0 falls off dramatically after only one CH=CH unit is at variance with our experimental data which show that a E,E-1,3-butadienyl bridge is effectively optimal. These differences in conclusions may arise from limitations of the ZINDO theoretical model, but are more probably related to the obviously limited similarity between a neutral Cr(CO)$_5$ unit and a dicationic Ru^{II} ammine center, the latter being a considerably stronger electron donor.

Theoretical Studies. To further probe and rationalize the unusual linear and NLO properties of our novel metallopolyene chromophores, we have also carried out MO calculations on the complex cations in salts **1**−**4** and **6**−**9**. Molecular first hyperpolarizabilities have been calculated by the finite field (FF) method that involves a double numerical differentiation of the dipole moment with respect to the applied electric field. Excitation energies E, transition dipole moments and ground and excited-state dipole moments have been calculated using

Table 5. Results of B3P86/LanL2DZ Calculations for the Electronic Transitions of the Complex Cations in Salts **1**−**4** and **6**−**9**[a]

parent salt	$\beta_0{}^b$ (10^{-30} esu)	E^c (eV)	$f_{os}{}^c$	$\mu_{12}{}^c$ (D)	$\Delta\mu_{12}{}^c$(D)	transition
1	112	2.57	0.37	6.19	21.17	HOMO → LUMO
		4.86	0.51	5.25	1.33	HOMO-3 → LUMO
2	112	2.56	0.48	6.99	26.07	HOMO → LUMO
		3.84	0.43	5.45	16.72	HOMO → LUMO+1
		4.01	0.49	5.69	6.22	HOMO-3 → LUMO
3	156	2.62	0.79	8.90	27.94	HOMO → LUMO
		3.39	1.06	9.10	3.48	HOMO-3 → LUMO
4	134	2.60	1.74	13.27	18.81	HOMO → LUMO
		3.07	0.57	6.99	10.94	HOMO-3 → LUMO
6	192	2.34	0.50	7.50	21.71	HOMO → LUMO
		3.80	0.17	3.40	1.76	HOMO → LUMO+2
		4.87	0.50	5.19	5.56	HOMO-6 → LUMO
7	259	2.34	0.58	8.07	26.97	HOMO → LUMO
		3.57	0.34	4.98	10.10	HOMO → LUMO+1
		3.99	0.73	6.96	4.41	HOMO-3 → LUMO
8	271	2.42	0.83	9.52	29.77	HOMO → LUMO
		3.31	1.14	9.95	6.57	HOMO-3 → LUMO
		3.54	0.13	3.14	1.53	HOMO → LUMO+1
9	212	2.46	1.58	13.01	25.03	HOMO → LUMO
		3.00	0.96	9.19	7.78	HOMO-1 → LUMO
		3.34	0.01	1.05	9.04	HOMO → LUMO+1

[a] Calculated in the gas phase using the optimized B3P86/LanL2DZ geometry. [b] Calculated using the FF method. [c] From TD-DFT calculations. The measured E_{max} values for the HE ILCT transitions are as follows (eV, in acetonitrile at 298 K): 4.63 (**1**), 3.97 (**2**), 3.50 (**3**), 3.16 (**4**), 4.88 (**6**), 3.99 (**7**), 3.48 (**8**), 3.16 (**9**).

the time-dependent density-functional theory (TD-DFT) approach. Although TD-DFT is known to yield a poor description of excitations involving charge-transfer,[36] it is the most accurate method that can be used on large molecules at an affordable computational cost. The choice of the B3P86 functional was based on the more accurate TD-DFT results provided by this functional when compared to the more widely used B3LYP.[37] The results of these calculations are presented in Table 5.

Although the extent of quantitative agreement is limited, the theoretical calculations generally predict the experimentally observed trends. The calculated molecular static first hyperpolarizabilities do not increase steadily on increasing the length of the π spacer, but reach a maximum at $n = 2$ (for the cations in **3** and **8**) and then decrease on passing to $n = 3$ (for the cations in **4** and **9**). The FF approach yields reasonable estimates of β_0 values, but does not provide an intuitive interpretation of the results. We have therefore also performed TD-DFT calculations in order to explore the excited electronic states of these molecules. Given that TD-DFT calculations give rise to a poor description of CT processes and that solvent effects have not been considered, the results of such calculations are expected to yield a qualitative explanation of the experimentally observed trends, rather than quantitative data. The results presented in Table 5 show that there are two common features in all of the compounds studied: the LE absorption is due in every case to a HOMO → LUMO transition, and there is also a HE absorption arising from a transition from an orbital below the HOMO (HOMO-3 in most cases, but HOMO-6 for **6** and HOMO-1 for **9**) to the LUMO. In a broad sense, the picture emerging from these calculations is similar to the model proposed for metallo-

(35) Kanis, D. R.; Lacroix, P. G.; Ratner, M. A.; Marks, T. J. *J. Am. Chem. Soc.* **1994**, *116*, 10 089−10 102. ZINDO−SOS calculations at a wavelength of 1907 nm gave $\beta_{vec} \times 10^{30}$ esu (n): −29.2 (0), −44.6 (1), −29.4 (2), −22.1 (3). Neither calculated MLCT maxima nor dipole parameters were quoted in this report.

(36) Tozer, D. J.; Amos, R. D.; Handy, N. C.; Roos, B. O.; Serrano-Andrés, L. *Mol. Phys.* **1999**, *97*, 859−868.
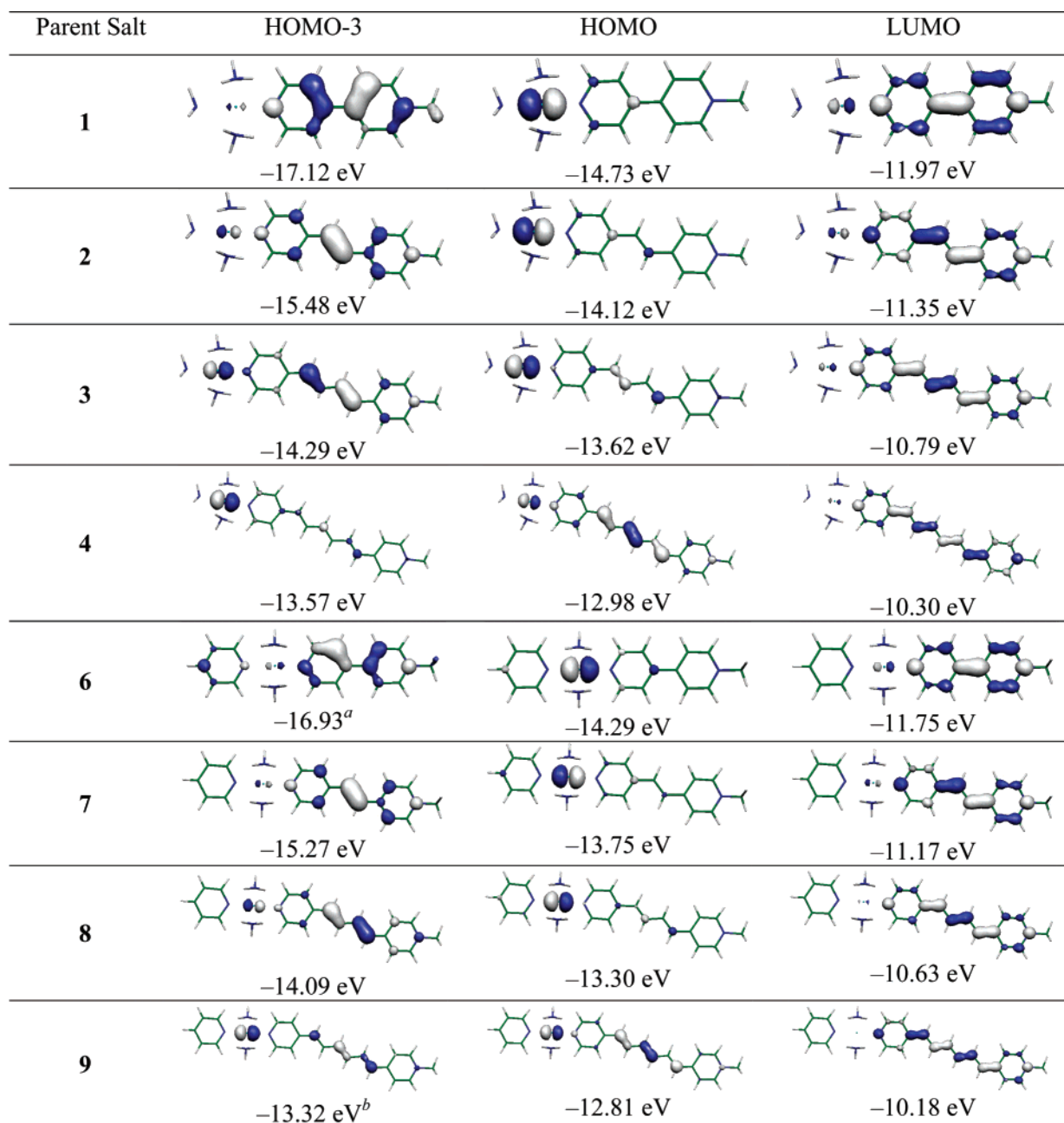(37) Wiberg, K. B.; Stratmann, R. E.; Frish, M. J. *Chem. Phys. Lett.* **1998**, *297*, 60−64.

Parent Salt	HOMO-3	HOMO	LUMO
1	−17.12 eV	−14.73 eV	−11.97 eV
2	−15.48 eV	−14.12 eV	−11.35 eV
3	−14.29 eV	−13.62 eV	−10.79 eV
4	−13.57 eV	−12.98 eV	−10.30 eV
6	−16.93[a]	−14.29 eV	−11.75 eV
7	−15.27 eV	−13.75 eV	−11.17 eV
8	−14.09 eV	−13.30 eV	−10.63 eV
9	−13.32 eV[b]	−12.81 eV	−10.18 eV

Figure 6. Illustrations of the 0.05 contour surface diagrams of the MOs involved in the LE (MLCT) and HE (ILCT) transitions for the complex cations in compounds **1**−**4** and **6**−**9**, calculated from TD-DFT. [a] HOMO-6. [b] HOMO-1.

cene D-π−A compounds,[32] involving a LE band assigned as MLCT or d → π* and a HE band regarded as ILCT or π → π* in character. This result also concurs with the Stark spectroscopic results (see earlier). Our calculations also predict that while the HE bands shift bathochromically on lengthening the π spacer, this is not the case for the LE bands which are rather insensitive to the length of the spacer and display an overall small hypsochromic shift when moving along the two series of compounds (**1** → **4** and **6** → **9**).

Quite surprisingly, these calculations predict that the change in dipole moment ($\Delta\mu_{12}$) caused by the LE transition decreases on passing from compound **3** to **4** and from **8** to **9**. An explanation of this result can be found based on the topology of the MOs involved in this transition (Figure 6). It can be seen that the HOMO, being essentially a Ru^{II} 4d orbital in compounds **1** and **6**, gains in π character along the two series of compounds

and consequently the LE transition usually considered as MLCT (d → π*) has some ILCT (π → π*) contribution that increases with the conjugation path length. Whilst theoretical calculations probably overestimate this effect (this decrease in $\Delta\mu_{12}$ is not observed experimentally; Table 3) it constitutes a possible explanation for the unexpectedly low β_0 values of the $n = 3$ homologues in these series of compounds. The calculations also predict that μ_{12} continually increases up to $n = 3$, in contrast to the experimental data which show that this parameter is maximized at $n = 2$ (Table 3). Concerning the excitation energy of the HOMO → LUMO band, the calculated HOMO−LUMO gap remains nearly constant (within 0.12 eV) along the two series of compounds, in manner similar to the predictions made for ferrocenyl chromophores by Barlow et al.[32] This phenomenon, together with the increased correlation on lengthening the π bridge already observed in oligo(phenylenevinylene) com-

pounds[30] that causes a decreased HOMO → LUMO contribution to the LE transition, is responsible for the observed hypsochromic shifts.

Concerning the HE transitions, the TD-DFT calculations reproduce the experimental excitation energies (measured at 298 K in acetonitrile) rather more closely than is the case for those of the LE bands (Table 5). This greater accuracy of prediction is probably due to the decreased CT character of these transitions when compared to the LE ones. The trends in E for the HE bands are entirely as expected, showing a red-shift on increasing the length of the conjugated spacer. It is noteworthy that the topology of the orbitals involved (Figure 6) shows an increased contribution of the Ru^{II} 4d orbital to the HOMO-3 and hence an increased MLCT character for the higher homologues in the two series of compounds. In contrast to E, the calculated values of μ_{12} and $\Delta\mu_{12}$ for the HE transitions do not agree well with the experimental data.

Finally, there is also a feature common to all of the pyridine complexes in **6**−**9**, consisting of a transition from the HOMO to an antibonding π orbital, generally LUMO+1 (LUMO+2 for **6**). The oscillator strength calculated for this transition increases on moving from $n = 0$ to 1, then decreases with increasing n. The corresponding absorption is observed only for compound **6** and assigned as having d → π*(py) character (Table 1), but is probably hidden by the more intense HE bands in the higher homologues. The contribution of this transition to the NLO responses of these compounds is expected to be unimportant due to its high excitation energy and low intensity.

Conclusion

We have presented the first combined, detailed, experimental and theoretical study on the effects of polyene chain extension on the linear absorption and NLO properties of metal pyridyl complexes. The phenomenon of blue-shifting of CT bands with the addition of CH=CH units has only been reported once previously, and the observed decreases in β_0 with extension

beyond 2 double bonds are unprecedented. A reasonable level of agreement is found between experiment and theory, and the unusual optical behavior can be attributed to the orbital structures of the complexes. The TD-DFT results show that the HOMO gains in π character along the two series of complexes and consequently the lowest energy transition usually considered as MLCT in character has some ILCT contribution that increases with the conjugation path length. Hence, our results clearly demonstrate that while the design criteria for metal-containing NLO chromophores may often be similar to those for purely organic molecules, this is certainly not universally true. It is interesting to speculate how changes in the relative electron donating/accepting strengths of the terminal groups in dipolar metallopolyenes may affect the orbital structure and hence the observed optical properties. For example, it may be anticipated that more strongly electron-accepting units such as 5-methylidene-1,3-diethyl-2-thiobarbituric acid will cause the drop-off in β_0 to occur after a value of n greater than 2. Continued systematic studies can be expected to uncover further interesting, and perhaps unexpected, differences between the optical behavior of novel transition metal-based NLO chromophores and that of their more thoroughly studied purely organic counterparts.

JA0315412